Journal of Archaeological Method and Theory (2019) 26:1327–1375
https://doi.org/10.1007/s10816-019-09411-3

Experimentally Derived Sedimentary, Molecular, and Isotopic Characteristics of Bone-Fueled Hearths

Tammy Buonasera, et al. *[full author details at the end of the article]*

Published online: 23 February 2019

Abstract

Molecular and isotopic analysis of sediments from archaeological combustion features is a relatively new area of study. Applications can inform us about ancient pyrotechnologies and patterns of animal exploitation in a wide range of human contexts, but may be particularly informative with regard to ancient hunter-gatherers. Our analyses of sediments from experimental bone and wood fires, and from controlled laboratory heating sequences, provide fine-grained data on the formation and location of biomarkers from pyrolyzed animal fats in hearths. Integrating microstratigraphic, molecular, and isotopic data can improve recognition of bone fires in archaeological contexts, perhaps even where bone preservation is poor. Experimental bone fires produced an upper layer of calcined bone above a thin layer of tarry black amorphous material coating mineral sediments. Mineral sediments beneath the black layer showed little alteration but high lipid content. Sampling for molecular and isotopic analysis should target the black layer as the bulk of pyrolyzed biomarkers are located here and stable isotope values are less affected than in the overlying layer of ash or calcined bone. The combined presence of certain symmetric and slightly asymmetric saturated long-chain ketones (14-nonacosanone, 16-hentriacontanone 16-tritriacontanone, and 18-pentatriacontanone), especially together with heptadecane (C_{17} *n*-alkane), are molecular indicators of the thermal degradation of terrestrial animal fat. Formation and relative dominance of these molecules in hearth sediments relates to the initial prevalence of specific precursor fatty acids and can provide broad separations between sources. We suggest that separations could be further supported and expanded by combining stable isotope analysis of the same compounds.

Keywords Hearths · Bone burning · Biomarkers · Stable isotopes · Micromorphology · Lipids

Thermal processing and combustion of animal bone, fat, and oil for food and fuel has been critical to human survival in a wide range of contexts. Fat is an important source of energy and allows for efficient use of protein in carbohydrate-poor environments (Outram 2002;

Electronic supplementary material The online version of this article (https://doi.org/10.1007/s10816-019-09411-3) contains supplementary material, which is available to authorized users.

Speth and Spielmann 1983). For equivalent weights, fat has more than twice the caloric value of carbohydrates or protein and provides a number of essential nutrients (Outram 2002; Speth and Spielmann 1983; Vehik 1977). Marrow fat is easily accessed by breaking open the medullary cavity of long bones of terrestrial mammals. This compact source of fat is widely consumed among many traditional societies (Outram 2001, 2002:75), and particularly among recent hunter-gatherers in a range of environmental contexts—from the Hadza in Tanzania to Inupiat peoples in the North American Arctic (Burch 1972; Binford 1978; Yellen 1991; Kent 1993; O'Connell *et al*. 1988).

On the other hand, bone grease, fat that has been rendered from cancellous and compact bone, requires a significant amount of effort and thermal energy (generally by boiling or simmering in water) to extract (Binford 1978; Church and Lyman 2003; Jones and Metcalfe 1988; Manne 2010, 2014; Munro and Bar-Oz 2005; Stiner 2003). Nevertheless, bone grease production from large terrestrial mammals has been an important component of many marginal economies, especially in high latitudes (Binford 1978; Burch 1972; Leechman 1951). In fact, the majority of lipids contained in mammalian bones are locked within the cancellous and compact portions the skeleton, rather than the more easily accessed medullary marrow (McCullough and Ullrey 1983; Pavao-Zuckerman 2011). Bone grease is a nutrient rich, calorically dense, portable food. It is also useful for the storage and preservation of dried meat products such as pemmican (Frink and Giordano 2015; Karr *et al*. 2010; Leechman 1951). Adding fat to lean, dry meat also helps to increase the nutritional quality of such foods, providing fat soluble vitamins and protein-sparing calories (Speth and Spielmann 1983; Vehik 1977).

The use of bones as fuel for heat and light has also been described in diverse temporal and cultural contexts, but typically in climates that are very cold (Crass *et al*. 2011; Darwent 2001; Kedrowski *et al*. 2009; Odgaard 2003; Schiegl *et al*. 2003; Villa *et al*. 2002, 2004; Villagran *et al*. 2013). A number of factors affect decisions to process cancellous and compact bone for grease versus burning it to provide heat and light. Certainly, the absence of efficient technologies for long-term boiling (*e.g.*, during the Middle Paleolithic) would be a significant deterrent to bone grease preparations (but see Costamagno 2013; Lupo and Schmidt 1997). Yravedra and Uzquiano (2013) note that bone burning at Middle Paleolithic sites in northern Spain appears to have been commonplace. These authors propose that burning bone may have served a dual purpose, providing an additional source of fuel as well as cleaning up refuse. In the absence of boiling technologies for rendering bone grease, especially in cold and fuel-poor settings, the most advantageous treatment of bone refuse may have been to burn it for additional light and heat.

The availability of other sources of edible fats and the abundance of woody fuels (or other alternatives, such as large herbivore dung) in the environment are also crucial factors affecting the value of bones as fuel (Outram 1999, 2002). If other sources of fat are not limiting for survival and are more easily acquired than fats trapped in the cancellous and compact portions of bone, there would be little reason to render grease from bones (Outram 2002). In these situations, greater benefit might also be gained by exploiting the fuel value of bones. Bones from animals that have already been butchered, transported, and consumed require little or no additional processing to use as fuel, so negligible cost is involved. Why not harvest the last bits of energy remaining in a carcass as heat?

Previous research suggests that fires fueled predominantly by bone could be missed in the archaeological record. This is because when defining "hearths," researchers typically apply expectations for thermally altered sediments based on data from predominantly wood-fired examples. This is especially true in sediments where the most obvious indicator of a bone-fueled fire, namely the bone itself, is poorly preserved (Kedrowski *et al*. 2009; Crass *et al*. 2011). However, in such contexts, pyrolyzed lipids can provide basic information on the presence of burned animal fats and possibly identify general types of animal sources. In sediments where bone is better preserved, contextualized analysis of lipids in hearth deposits can provide additional information about the use and processing of certain animal products as food or fuel, including molecular clues about the sequence and primary location of burning. The ability to identify the presence of different types of animal fats, mixtures of animal and plant lipids, and to contextualize this within the sedimentary structure of a variety of combustion features, would provide an important means of understanding fuel use and fire technologies in past societies.

The present study is concerned with improving our ability to identify and locate inputs from animal fats in anthropogenic combustion structures using molecular analysis, compound specific stable isotope analysis (CSIA), and soil micromorphology. Combining molecular and isotopic analysis of sediments and pyrolyzed char from archaeological combustion features is a relatively new area of study (Buonasera *et al*. 2015; Choy *et al*. 2016; Heron *et al*. 2010; March 2013; March *et al*. 2014) and microcontextualized biomarker studies are rare (Sistiaga *et al*. 2014). Applications have the potential to inform us about ancient pyro-technologies and patterns of animal exploitation in a wide range of human contexts, from traditional farming societies to Paleolithic hunter-gatherers. The research presented here provides information on the formation and location of biomarkers from pyrolyzed animal fats in hearth sediments. We also discuss experimental data regarding thermal alterations to compound specific stable isotope values in hearth sediments. These data improve our understanding of conditions and locations conducive to the formation of pyrolytic biomarkers in hearth structures. This can help us interpret behavioral information and guide us in future sampling and analysis of sediments from archaeological combustion features.

Brief Review of Molecular and Stable Isotope Studies of Animal Fats in Archaeological Hearth Deposits

Organic residue studies of ancient hearth sediments date from at least the late 80s (March *et al*. 1989; March 1999; Rottländer 1989, 1991). However, the pace of this research is increasing as access to sensitive analytical instrumentation improves, techniques of organic residue analysis mature, and fire and cooking technologies are forefronted in human prehistory (Buonasera *et al*. 2015; Choy *et al*. 2016; García-Piquer *et al*. 2018; Kedrowski *et al*. 2009; Lejay *et al*. 2016; Lucquin 2007, 2016; March 2013; March *et al*. 2014; Prost *et al*. 2011). Our intent here is not to provide an exhaustive historical review, but to discuss the current state of knowledge regarding molecular and isotopic identification of animal fats in hearths. Toward that end, the works discussed below provide a foundation for the research questions addressed in the remainder of this paper.

Our review starts in central Alaska, where a series of dark smears and burned fat-encrusted residues, along with an absence of traditional hearth structures (charcoal and ash overlying a reddened substrate), were observed in the oldest component (c. 14,500–14,000 calendar years BP) of the Swan Point site. Environmental proxies for this component indicated a steppic environment that supported large herbivores, but where woody fuels may have been scarce (Crass *et al.* 2011; Holmes 2001; Kedrowski *et al.* 2009). This situation prompted experiments into the feasibility and archaeological signature of bone burning in the absence of wood (Crass *et al.* 2011; Kedrowski *et al.* 2009). Results of these experiments indicated that bones can be burned without woody fuel, using either grass or herbivore dung as an ignition source. The authors found that maintenance of bone fires using only additional bone was possible but required more care than a typical wood fire (Crass *et al.* 2011:194).

Kedrowski *et al.* (2009) used proportions of saturated fatty acids[1] and physical similarities between the experimental fire sediments and archaeological features to identify burned Swan Point sediments as the remains of fires fueled by bones of large terrestrial herbivores. Subsequent studies have focused on more robust molecular means of identifying animal fats in archaeological sediments, such as combining lipid biomarkers and stable C and N isotopes. Importantly, Kedrowski *et al.* (2009) also quantified the substantial amount of lipids in their 14,000-year-old hearth samples. Several ancient hearth samples had a milligram or more per gram of sediment (p. 116). This remarkably high concentration of fat, also detailed in the experiments presented here, may itself be a hallmark of bone burning.

In a different study, based in Arctic Norway, Heron *et al.* (2010) combined lipid biomarkers and bulk $\delta^{13}C$ and $\delta^{15}N$ analysis to test whether cemented sediments in ancient slab-lined pits contained evidence for the rendering of marine animal fats. The authors note that hundreds of slab-lined elliptical or rectangular pits, dating between 0 and 1200 A.D., are known from coastal sites in Arctic Norway. A variety of materials were analyzed from the pits, primarily cemented organic residues but also charcoal, non-charred sediments, and fire-cracked rocks. The cemented organic residues were described as a sand and gravel matrix cemented by brownish-black organic material. Of the four types of materials analyzed, charcoal and cemented organic residues were found to contain many of the same lipids, and also had the highest concentrations of lipids. Lipid biomarkers in these materials were largely consistent with aquatic resources (Heron *et al.* 2010).

Heron *et al.* (2010) also reported that the amount of nitrogen in the lipid-rich cemented organic residues and in marine reference fats was much lower than the amount of carbon, with many C:N ratios substantially higher than 100:1. Due to the low amounts of nitrogen, they noted that $\delta^{15}N$ values could not be reliably determined in most cases (Heron *et al.* 2010: Table 2). Bulk δ^{13} C values, on the other hand, were deemed informative and indicated input from marine animals. Although bulk $\delta^{13}C$ values represent a mixture of all organic sources in a sediment, and archaeological sediments can contain variable amounts from many different materials (*e.g.*,

[1] Although proportions of fatty acids can be useful for identifying modern fats, used in isolation, they are not a reliable means of identifying sources in archaeological materials (Heron and Evershed 1993). This is due to differences in the preservation of fatty acids of different chain lengths and degrees of unsaturation based on solubility and reactivity (March *et al.* 2014:23; Steele *et al.* 2010).

carbohydrates from woody fuels and plant remains, carbon from bone collagen and other proteins, or carbon from fats), the signal from the very high fat content was dominant in this case.

In a more recent Alaskan application, Buonasera *et al.* (2015) used a combination of lipid biomarkers and $\delta^{13}C$ values for two fatty acids to identify a marine source of burned, fat-encrusted sand from Arctic Small Tool tradition (ASTt), Norton, and Thule sites along the west coast of northern Alaska. Biomarkers targeted for analysis were the same as those used in the prior Heron *et al.* (2010) study: ω-(*o*-alkylphenyl) alkanoic acids 18, 20, and 22 carbons long (products of pyrolysis), as well as certain isoprenoid fatty acids (non-pyrolytic biomarkers of aquatic organisms). The pyrolysis products, ω-(*o*-alkylphenyl) alkanoic acids 18, 20, and 22 carbons long (APAAs) have been shown to form from highly unsaturated fatty acids of corresponding chain length at temperatures above 270 °C (Copley *et al.* 2004; Evershed *et al.* 2008; Hansel *et al.* 2004). Highly unsaturated compounds are not likely to survive archaeological time,[2] so these pyrolysis products do two things: (1) they inform us of the prior unsaturated character of the lipid source, and (2) they tell us that the lipids were exposed to high temperatures.

Molecular data were then combined with compound specific $\delta^{13}C$ values for two fatty acids, $C_{18:0}$ and $C_{16:0}$, which are typically the most abundant saturated fatty acids in archaeological lipid residues. Focusing on $\delta^{13}C$ values of specific lipids rather than bulk $\delta^{13}C$ values of burned sediments can help to avoid effects of large carbon inputs from woody fuels, which are primarily carbohydrates (cellulose, hemicellulose, and ligands). This last point highlights the importance of considering whether the major source of carbon in an organic residue is lipid, carbohydrate, or protein because lipids have lower $\delta^{13}C$ values than proteins or carbohydrates from the same organism due to additional fractionation during biosynthesis (DeNiro and Epstein 1977; Logan *et al.* 2008; Ryan *et al.* 2012).

This combination of molecular data and compound specific $\delta^{13}C$ values provided strong evidence for the earliest dated use of marine resources by people using ASTt technologies in northwestern Alaska. Yet, although the sediments were radiocarbon dated and in direct association with ASTt technologies, little else is known about the way these resources came to be burned. Were bones and/or oil burned as a fuel source, or are the residues related to food processing activities? Are combustion-related materials in their primary context of formation, or were they redeposited? To better understand the manner in which marine animal fats were incorporated in these early combustion features, the authors recommended that future molecular and isotope studies of burned-cemented sediments in northern Alaska include micromorphology of intact combustion features.

In another recent northern study, Choy *et al.* (2016) combined bulk $\delta^{15}N$ values with compound specific $\delta^{13}C$ values for $C_{18:0}$ and $C_{16:0}$ fatty acids in a concentration-dependent Bayesian mixing model to identify organic input from anadromous salmon in late Pleistocene hearth deposits from interior Alaska. Their mixing model incorporated compound specific $\delta^{13}C$ values of the two saturated fatty acids along with bulk

[2] Lipids with one or more double bonds in the carbon chain, such as unsaturated fatty acids, or alkenes, are not good candidates for long-term preservation. The carbon-carbon double bond has a much higher reactivity than those on saturated carbons (Cranwell 1981; McMurry 1992:149–150).

$\delta^{15}N$ values from modern samples of muscle tissues to distinguish three groups of organisms: marine (anadromous salmon), freshwater (freshwater fish and aquatic birds), and terrestrial (terrestrial mammals and terrestrial birds). Contrary to the Heron *et al.* (2010) study, these authors found that bulk $\delta^{13}C$ values were not useful for identifying potential animal contributions in their hearth samples because bulk $\delta^{13}C$ values were quite similar between hearths. This is possibly because the organic C content of their archaeological hearth sediments was dominated by the (non-lipid) products of woody fuel. To get around this problem, Choy *et al.* (2016) used the compound specific $\delta^{13}C$ approach focused on values of $C_{18:0}$ and $C_{16:0}$ fatty acids. This allowed Choy *et al.* (2016) to isolate the organic content most likely to contain large contributions from animal fats, rather than the bulk content which was more likely to be dominated by carbon derived from (non-lipid) woody fuels. Modeling these compound specific data along with bulk $\delta^{15}N$ values, the authors were able to identify OM input from anadromous salmon in central Alaskan hearths dating between 13,200 and 11,500 Cal BP (Choy *et al.* 2016; Halffman *et al.* 2015).

In addition to the above applications, two recent studies have employed field experiments to begin unraveling molecular inputs and alterations to hearth sediments with the burning of plant and animal fuels. March *et al.* (2014) provided an important generalized overview of major changes in the lipid fraction of soil organic matter (SOM) in natural sediments beneath hearths due to thermal alteration, fuel inputs, and cooking. Information was collected from experiments conducted at a range of temperatures and conditions as well as observations made from archaeological hearths in various settings. Over the course of laboratory heating from 100 to 600 °C, the authors noted that the distribution of *n*-alkanes from native organic material in the sediments was smoothed at progressively higher temperatures and the ratio of palmitic ($C_{16:0}$) to stearic ($C_{18:0}$) acid decreased (pp. 23–24). They reported that polyunsaturated and monounsaturated fatty acids declined rapidly from about 100 to 200 °C, followed by the loss of other compounds including alcohols, ketones, and alkanes at temperatures above 300 to 400 °C. By 600 °C, almost no original organic material remained. (It is assumed that heating experiments were performed solely in the presence of oxygen, where combustion reactions rather than pyrolysis would dominate.)

Along with this reduction in native SOM content, the authors noted that contributions from fuel and food residues could be very large and overwhelm remaining traces of original SOM. Lipid input from bones was differentiated from wood fuel by an absence of long-chain alkanes and poor preservation of sterols (cholesterol) for bone lipids. Lipid residues from cooking animal foods were also reported to include a variety of (unspecified) short and long-chain ketones, γ-lactones, and short-chain alkanes. Relative amounts of different lipid classes were not discussed, however, and little information was provided on the conditions of formation and occurrence of specific molecules.

More recently, Lejay *et al.* (2016) designed a controlled set of field experiments to analyze molecular products of bone and wood fires. Their results outline gross molecular differences in types of pyrolysis products found in bone and wood fires. Burned sediments were analyzed for lipid content *via* GC/MS and py (TMAH)-GC/MS (tetramethyl ammonium hydroxide) assisted pyrolysis coupled to GC/MS. Similar to March *et al.* (2014), aromatics, alkanes, alcohols, γ-lactones, and ketones are reported to occur, but specific molecules and relative amounts present in different samples and

sedimentary layers of the fire structures are not elucidated. Phenolic compounds and aromatic compounds were only detected in fires which consumed wood, while bone fires were associated with a series of *n*-alkane/alkene doublets, short-chain oxoacids and short-chain alcohols, γ-lactones, and long-chain ketones.

Although no temperature data were recorded, Lejay *et al.* (2016) used depth and degree of reddening as proxy information on heat transfer into the sediments. They reported the greatest degree and depth of thermal alteration (reddening and darkening down to 4 cm) beneath a bone fire (bone with a small amount of wood for ignition). The least amount of thermal alteration was observed beneath the wood fire (reddening 0.5 to 1.5 cm deep). These observations are interesting because they contrast with those reported by Kedrowski *et al.* (2009) and Crass *et al.* (2011), who describe less heat transfer and a lack of reddening in sediments beneath their bone fires.

Overall, studies on the molecular and isotopic content of hearth sediments are picking up pace. Recent experimental contributions by March *et al.* (2014) and Lejay *et al.* (2016) provide a foundation for additional molecular work on identifying fuels and other organic contributions. Distributions of specific molecules in hearth sediments and better understanding of the mechanisms of formation are needed to improve identification of bone fires and specific animal fuels. We also need more information on temperatures routinely reached in sediments beneath different types of fuels. Temperature data and associated visible alterations of sediments may be crucial for updating sedimentological criteria used to define hearths. Further, none of the studies listed above have addressed potential thermal alterations to stable carbon isotope values in hearth sediments. To improve reliability of identification criteria, it is necessary to better understand potential isotopic shifts due to thermal treatments (Poole *et al.* 2002).

Goals of the Current Study

With these prior experiments as backdrop, we sought to replicate and expand molecular and isotopic data for predominantly bone-fueled versus wood-fueled fires under more controlled conditions. Our purpose was to acquire detailed and specific molecular information in combination with temperature distributions and microstratigraphic information. Though we have general ideas about differences in wood and bone fires, more information will allow us to select specific biomarkers and combine this with isotopic values and physical criteria. We also wanted to know the best materials and locations of the fire structures to sample for molecular and isotopic analyses. Together, this information will improve identification of source materials and analysis of formation processes.

In addition to the need for a better understanding of biomarker formation and location, and possible thermal affects to stable isotope values, we wanted to explore a contradiction that exists in the literature describing the transfer of heat to sediments beneath bone fires. Kedrowski *et al.* (2009) and Crass *et al.* (2011) conducted laboratory and field experiments in which they burned bone using only grass as tinder. They reported that the sediments under the fire remained relatively cool to the touch, little or no ash was produced, and upon removing the fragments of burned and calcined bone, only a layer of blackened and fat-encrusted sand was present on the surface. They observed no reddening or other alteration of the substrate beneath the black, crusted

sand. In contrast, Lejay *et al*. (2016) reported an increase in the depth of reddening beneath fires that contained greater proportions of bone to wood. While other factors such as moisture and mineral content play a role, all else being equal, higher temperatures should produce more reddening. Given this apparent contradiction, and an absence of reported temperatures, we wondered: do bone fires transfer more or less heat to underlying sediments? Are sediments beneath a bone fire affected differently than those beneath a wood fire?

Since Kedrowski *et al*. (2009) and Crass *et al*. (2011) conducted their burning experiments on sand, it is possible the lack of reddening observed could be due to a low amount of iron in the substrate. On the other hand, their observations of cooler temperatures under bone fires versus wood fires are in agreement with experiments performed by Théry-Parisot (2002) who noted that bone fires produced a substantial amount of convective and radiant heat but were very poor conductors of heat. (Conduction is the transfer of heat between solids that are in contact, while convective heat is the movement of a heated gas or liquid, and radiant heat is a form of electromagnetic energy.)

To increase our potential for gaining information about the use of different animal sources as food or as fuel, we need greater specificity identifying products of pyrolysis and effects on stable carbon isotope values in hearths. Additionally, to better understand differences in formation processes, and to improve sampling and analysis, it is crucial to integrate stratigraphic and micromorphological information with molecular and isotopic information. Stable isotopes can be very useful for analyzing sources of animal fat, but are more powerful when combined with information that can shed light on the type and extent of fuel mixing, post-depositional alterations, and the contemporaneity of organic materials in hearth layers with living floors. In combination, molecular, isotopic, and microstructural data can define important behavioral information associated with the use of these features.

Laboratory and field experiments were conducted to address the following specific goals:

1) Compare the footprint and profile of predominantly bone fires to wood fires
2) Compare the heat transfer in sediments during predominantly bone fires to wood fires
3) Track the location and movement of lipids in sediments beneath the fires
4) Identify specific biomarkers of burned animal fats, their location, and conditions of formation
5) Test the thermal stability of $\delta^{13}C$ values in fatty acids

Methods

Experimental Fires

Experimental fires were conducted in the field at the Laboratorios de Calidad de la Construcción, Consejería de Obras Públicas, Gobierno de Canarias (Fig. 1). To avoid contributions from existing SOM and to maintain the same starting conditions, each fire was made on a freshly prepared mineral sediment consisting of crushed and compacted basalt that ranged from small pebble to silt-sized particles. An artificial basalt sediment

was selected because an abundant supply could easily be produced for us at the Laboratorios de Calidad de la Construcción, which is located on the volcanic island of Tenerife. Basalt is a common igneous material and component of volcanic soils. Control samples for residue analysis and micromorphology were taken prior to the firing experiments.

The fires were made on flat, unmodified surfaces in an exposed setting. Temperatures on the sediments beneath the fire were monitored with a Lutron 4-channel thermometer (model: TM-947SD). Thermocouples were buried in the sediment prior to firing and temperatures were recorded continuously over the duration of each fire. The probes were placed in the center portion of the fire and stacked in the same horizontal position at the following intervals: 0 cm (at the surface), 1 cm, 3 cm, and 5 cm below the surface. The total weight of fuels was kept similar for each experiment (~ 5.0 kg). The pine wood fire burned only pine wood, while the bone fire burned approximately 80% fresh cow bone and 20% pine wood. Local pine wood (*Pinus canariensis*) was purchased dried and pre-cut from a local firewood business. The wood was mostly bark-free and ranged in size from approximately 5 cm × 15 cm to 10 cm × 20 cm. Cow bones (*Bos taurus*) were fresh and were obtained from a local butcher. The bone material consisted of long bones, vertebrae, and ribs from a recently butchered cow that were cut into pieces ranging between 10 and 20 cm at the longest dimension. Prior to burning, exterior surfaces of the bones were cleaned of muscle and fat as much as possible, but some of these tissues remained.

Micromorphological Analysis

Soil micromorphology is a common technique used in the microstratigraphic analysis of natural and archaeological soils and sedimentary deposits to characterize their

Fig. 1 Artificial crushed basalt sediment bed, prepared at Laboratorios de Calidad de la Construcción, Consejería de Obras Públicas, Gobierno de Canarias

formation through microscopic observation of their components and their spatial arrangement (Courty *et al*. 1990; Stoops and Vepraskas 2003). Intact blocks of sediment (approximately 10 cm at each side and 20 cm long) were collected from the experimental combustion structures, along with one control block taken before the fires. The blocks were processed into petrographic thin sections in the AMBI Lab, University of La Laguna, Tenerife, Spain. First, the blocks were oven-dried at 60 °C for 48 h in a laboratory oven. Subsequently, they were embedded in a 7:3:0.6 mixture of polyester resin (Palatal strained resin UN1866, TNK composites), styrene (Styrene monomer (CAS: 100-42-5) UN2055, TNK composites), and a catalyzer (methyl-ethyl-ketone (Luperox, CAS: 78-93-3), TNK composites). Once hardened, the blocks were cut into 1-cm-thick slabs using a Euro-Shatal M31100 radial saw, which were then glued onto 9 cm × 6 cm glass slides. These were reduced to a thickness of 3 mm using an ATM Brillant-220 precision cutting machine and to 30 μm using a G&N MPS-RC-Geology grinding machine. The resulting thin sections were observed under plane and crossed polarized light using a Nikon AZ-100 polarizing microscope with 1–100 magnifications.

Laboratory Heating Experiments

Heating experiments were conducted in the lab with samples of cow marrow fat combined with crushed basalt matrix (the same matrix that was used for the outdoor fires). Bone marrow fat used in the heating experiments was obtained from the distal portion of a fresh beef (*Bos taurus*) femur purchased from a local grocery store in La Laguna, Tenerife. All laboratory heating experiments used marrow fat from this same source, although this was from a different individual animal than the outdoor fire (see above). Because significant changes in the appearance of pyrolysis products occur around or above 300 °C (Maher and Bressler 2007; Maher *et al*. 2008; Nawar 1969; Raven *et al*. 1997; Schwab *et al*. 1988), different sub-samples of marrow fat from the same portion of the same bone were heated for 1 h each at 300 °C, 350 °C, and 400 °C in a muffle furnace.

Heated samples were prepared by placing marrow fat (~ 0.5 g) on a layer of basalt sediment (~ 9.5 g) in a ceramic crucible covered with aluminum foil to reduce exposure to oxygen during heating (Wiedemeier *et al*. 2015; Wiesenberg *et al*. 2009). Although oxygen was limited to some extent, the covers were not air-tight. Contents were brought to the selected temperature as rapidly as possible (26 °C/min) and maintained at the selected temperature for 60 min. Afterward, samples were allowed to cool in the oven until they reached room temperature. After cooling, samples were removed from the crucible, wrapped in foil, placed inside plastic bags, and stored in the refrigerator until they were extracted and analyzed. For comparisons to fresh materials, samples of unheated cow marrow fat, pine wood, and unused basalt sediment were retained for analysis.

Molecular and Isotopic Analysis

Extraction, Fractions, and Derivatization

Samples were allowed to dry at room temperature or in a laboratory oven at 25 °C. Dried samples were ground to a powder using an agate mortar and pestle and extracted

2× using 20 mL of dichloromethane (DCM) and methanol (2:1) with 20 min sonication each time. Sample quantities are provided in Table 1. The two extracts were combined, for a total of 60 mL, centrifuged at 4700 RPM for 20 min, and filtered through glass wool. The filtered extract was then dried under a gentle stream of nitrogen and reconstituted in 3 mL of DCM. This was the total lipid extract (TLE). A small portion (100 μL) of the TLE was then dried and fatty acids (free fatty acids as well as those from tri-, di-, and monoacylglycerols) were trans-esterified to fatty acid-methyl esters (FAMEs) to increase their volatility for GC/MS analysis. FAMES were made by adding 5 mL of 4% H_2SO_4 in methanol (MeOH) to the dried aliquot and tightly capping the vial. Contents were then heated at 80 °C for 60 min. Following this, the FAME mixture was neutralized with a saturated sodium bicarbonate solution and FAMES were extracted with 3 mL hexane (3×). Hexane extracts were combined, dried under nitrogen, weighed, and diluted in an appropriate amount of dichloromethane. This was the FAME total lipid extract.

The remainder of the original TLE was loaded onto a silica column (1 g silica—pore size 60 Å, 70–230 mesh, 63–200 μm; and 0.1 g sand—50–70 mesh particle size) and five fractions were eluted with solvents of increasing polarity: F1-alkanes, F2-aromatics, F3-ketones, F4-alcohols, F5-fatty acids. Methods for separating and collecting fractions follow those described in Jambrina-Enríquez *et al.* (2018). The first three fractions (alkanes, aromatics, and ketones) were dried under nitrogen, reconstituted in an appropriate amount of DCM, and analyzed without derivatization. Analysis focused on F1, F2, and F3 because these types of molecules have greater potential for long-term preservation, and because alcohols and fatty acids were visible in the TLE. However, the remaining fractions were retained for future analysis.

Table 1 Distributions of molecular components in the cow bone fire (EF1) layers and pine wood fire (EF2) layers

Experimental fires and layers	Alkanes (μg/g)	Aromatics (μg/g)	Ketones (μg/g)	TLE (μg/g)	Sample wt. (g)	Sample description
EF1 white layer	0.01	NMC	NMC	14.38	2.27	Calcined bone and ash
EF1 black layer	5.71	0.81	2.61	1855.33	4.98	Crushed basalt sediment with blackened organic material coating mineral surfaces. Below the white layer
EF1 brown layer	0.75	0.03	1.15	1308.41	5.50	Crushed basalt sediment beneath black layer, darker brown appearance due to wetting effect from lipid contribution. Not visibly blackened
EF2 white layer	NMC	NMC	NMC	0.12	12.51	Ash with some charcoal, above blackened basalt sediment
EF2 black layer	NMC	NMC	NMC	0.38	13.82	Blackened crushed basalt sediment at ground surface, below the white layer

NMC, no measurable components

Prepared samples were stored at − 20 C in glass vials with foil-lined Teflon caps. Appropriate dilutions were made and an internal standard (5-α-androstane − 2000 mg/L in DCM, purity ≥ 99.9%, Sigma-Aldrich for F1, F2, and F3, and C19:0 purity ≥ 98%, Sigma-Aldrich for the FAME TLE) was added to all samples prior to analysis. Blank samples were prepared along with several batches to test for laboratory contamination.

Solvents and reagents were HPLC grade or better and provided by Scharlau (Barcelona, Spain), Sigma-Aldrich (Madrid, Spain) and Honeywell (Seelze, Germany). Glassware and laboratory utensils were automatically cleaned with an alkaline laboratory cleanser, thoroughly rinsed with DI water, and then baked in a kiln at 450 °C for 10 h. Items that could not be placed in the kiln were cleaned in an ultrasonic bath with Derquim + universal detergent (Panreac-AppliChem, Barcelona, Spain) for 10 min, then rinsed with tap water for 2 min and with Milli-Q water (Milli-Q gradient system A10 Millipore, Bedford, USA) for 10 min more. Finally, this material was rinsed five times with MeOH and dried at room temperature.

GC/MS Analysis

Samples, 1 μL, were analyzed on an Agilent 7890B GC coupled to a 5977 MSD single quadrupole mass spectrometer (MS) with an electron impact interface. Two different columns and several temperature programs were used as described below. First, all samples and fractions were run using an HP-5 ms column, (5% phenyl) methylpolysiloxane (30 m × 0.250 mm ID, 0.25 μm film thickness). FAME TLEs, F1 and F2 (alkanes and aromatics), and F3 (ketones) were run at an initial oven temperature of 70 °C (held for 2 min), then temperature was increased to 140 °C (heating rate of 12 °C/min) and finally increased to a temperature of 320 °C (heating rate of 3 °C/min) and held for 15 min. Helium flow was set at 1 mL/min for FAMEs and 2 mL/min for F1, F2, and F3. The multimode injector was programmed at 70 °C for 0.85 min and then the temperature increased to 300 °C at a heating rate of 720 °C/min. Injections were made with split ratios of 2:1 for FAMEs and F3 and 5:1 for F1 and F2.

To improve the sensitivity of detecting and quantifying long-chain ketones, all ketone fractions (F3) were also run on a DB-1 column, 100% dimethylpolysiloxane (30 m × 0.32 mm ID, 0.25 μm film thickness), with the following program. The temperature was initially set at 50 °C, then increased at a heating rate of 15 °C/min to 320 °C and held for 25 min. Injections were made in splitless mode at 300 °C and He flow was set at 1 mL/min.

The MS was operated in full scan mode (*m*/*z* 40–1000) for all samples and also in SIM mode (*m*/*z* 239, 255, 267, 283) for ketones. The transfer line was set at 280 °C, the ion source at 230 °C (electron ionization energy of − 70 eV), and the quadrupole at 150 °C.

HP MassHunter software was used to operate the equipment and integrate peaks. Peaks were identified based on characteristic ions, reference to the NIST Mass Spectral Database v.14, and by comparison of retention times and mass spectra of authentic standards run under the same conditions. Supelco 37 FAME Mix (C4:0–C24:0 concentration in DCM varied from 200 to 600 mg/L, purity from 96.8 to 99.9%, Sigma-Aldrich), a mixture of 37 fatty acids common to food sources, was used as authentic standards for FAMES. Alkane calibration standard mixture C8-C40 (500 mg/L of each alkane in DCM, purity ≥ 90.1%) was used to identify alkane retention times. Authentic standards for long-chain ketones were purchased from Tokyo Chemical Industry (16-

hentriacontanone, purity > 95%), Alfa Aesar (18-pentatriacontanone, purity > 85%), or synthesized by Dr. José Antonio Palenzuela López, Instituto Universitario de Bio-Orgánica Antonio González, Universidad de La Laguna, Tenerife (14-nonacosanone). Mass spectra of long-chain ketones were also compared to predicted fragmentation patterns discussed in Vajdi *et al*. (1981).

Quantification

Many samples were run in duplicate, or more times if the concentration was very low. Lipid totals for each sample fraction were calculated by comparing the total ion count for a known amount of internal standard to the total ion count of all lipids detected in the sample. For alkanes, quantification was also carried out using the four most intense fragment ions (*m*/*z* 43, 57, 71, and 85, and *m*/*z* 67, 95, 81, and 245 for IS). It is worth mentioning that this estimation of concentrations can be further improved through matrix-matched calibration (Herrera-Herrera and Mallol 2018). The signal of compounds, and particularly lipid biomarkers, can be affected differently by the presence of the sample components other than the target analyte when instrumental techniques are used (see references in Herrera-Herrera and Mallol 2018). In this study, other than calcined bone, the matrix (crushed basalt) remained constant for all experimentally heated and fired samples.

GC-IRMS Analysis

FAME TLEs and some alkane fractions were analyzed on a TRACE 1310 GC, linked to a Delta V isotope ratio MS (IRMS) *via* a temperature converter GC Isolink II and a Conflo IV interface to measure $^{13}C/^{12}C$ isotope ratios for specific fatty acids and alkanes. Samples, 1 μL, were analyzed using a Trace Gold 5-MS (Thermo Scientific) fused silica capillary column, (5%-diphenyl)-dimethylpolysiloxane (30 m length × 0.25 mm i.d., 0.25 μm film thickness) programmed at 70 °C for an initial isothermal period of 2 min, followed by an increase to 140 °C (rate 12 °C/min) and held for 2 min, and finally the temperature was increased to 320 °C (rate 3 °C/min) and held for 15 min. Helium flow (as carrier gas) was set at 1.5 mL/min. Injections were made in spitless mode by means of a programmed temperature vaporizing injector (PTV). The temperature of the injector was initially set at 60 °C (held 0.05 min) and then increased to 79 °C at a rate of 10 °C/s and held for 0.5 min during an evaporation step. Finally, a cleaning step was carried out increasing the temperature to 325 °C (held 3 min) at a heating rate of 10 °C/s. The combustion reactor was maintained at a temperature of 1000 °C during all the analyses. $\delta^{13}C$ values were normalized to the Vienna Pee Dee Belemnite (VPDB) scale using a *n*-alkane type A6 mixture (*n*-C_{16} to *n*-C_{30}) or a fatty acid ester F8–3 mixture ($C_{14:0}$ methyl ester to $C_{20:0}$ ethyl ester) of known isotopic composition, both from Arndt Schimmelmann (Biogeochemical Laboratories, Indiana University). The standard deviation of carbon isotope measurements was better than ± 0.5‰. Isodat 3.0 software (Thermo Scientific) was used for controlling the equipment and for data acquisition and processing. For FAMEs, since the methyl group introduced during derivatization contributes to the isotopic composition, a correction to obtain the true value for fatty acids was made using the following equation (because little or no fractionation is expected during this derivatization) (Regert 2011).

$$\delta^{13}C_{FA} = \frac{(C_n + 1)\delta^{13}C_{FAME} - \delta^{13}C_{MeOH}}{C_n}$$

where $\delta^{13}C_{FA}$ is the value for the underivatized fatty acid, C_n corresponds to the number of carbon atoms in the fatty acid, $\delta^{13}C_{FAME}$ is the value for the fatty acid-methyl ester, and $\delta^{13}C_{MeOH}$ corresponds to the value for methanol used for the methylation. The $\delta^{13}C_{MeOH}$ values were obtained at the Stable Isotope Facility at the University of California, Davis.

Results and Discussion

Field Observations and Heat Profiles of Experimental Bone and Wood Fires

Field Observations During the Bone Fire (EF1)

The bone fire (EF1) was conducted on 22 May, 2017 (Fig. 2). The day was overcast and the temperature at the start of the fire was 19.4 °C (67 °F) with a light breeze at 9.7 km/h (6 mph), NNE. Temperatures remained about the same over the duration of the fire but winds picked up considerably after the first hour with 29.0 km/h (18 mph) gusts. Light precipitation began to fall just as we were wrapping up and pulling the thermocouples from the sediment. Sediment moisture at the start of the fire (measured gravimetrically) was 0.85% in the first cm and 2.75% at 5 cm.

We started the fire with a couple of handfuls of pine wood splinters and shavings (~ 100 g) mixed with four larger pieces of pine wood (~ 400 g). Once this was burning steadily, two pieces of cow long bones (~ 20 cm × 10 cm each, ~ 700 g total) were added. This caused the flames to subside. We were able to revive the flames with some splinters of a bone that had been broken open with a sharp heavy stone to expose the marrow. Adding a few splinters of bone and a little fatty marrow kept the flame going. We also found that adding larger pieces of marrow immediately smothered the flames.

Although large pieces of fresh fatty medullary marrow may have been eaten on the spot by foragers, our goal was to maintain a mostly bone-fueled fire and observe how all parts of the bone affected the fire. Our observations suggest that adding pieces of pure medullary marrow to fires would have been undesirable for pyrotechnical reasons as well as dietary ones. In fact, animal fat, which is composed of triglycerides as well as water and other impurities, is not highly flammable and must reach temperatures of over 300 °C to sustain ignition (Shahidi 2005). This temperature threshold is easier to achieve when smaller amounts of fat are spread over a larger surface area and exposed to flame. To some extent, the matrix of the bone may serve a function similar to a wick in in oil lamp, increasing the surface exposure and rate of heating of the fat.

Additional bones, including vertebrae with portions of ribs, were cracked and added at intervals when we noted the flames beginning to subside. The fire burned in this way with only cracked portions of bone added, for almost 90 min. Once the fat in the bone was heated and ignited, it continued to burn. By late morning, however, the wind had increased to 29.0 km/h (18 mph) gusts, and we had difficulty maintaining the flame. Eventually, the flame went out and we were unable to restart the fire without adding wood. At this point, another ~ 500 g of wood was used over the next 50 min in attempts

Fig. 2 Early phase of the cow bone fire (EF1) on the artificial basalt sediment. Thermocouples were placed in a central area of the fire at the surface (0 cm), 1 cm, 3 cm, and 5 cm below the sediment surface

to relight the fire. After flames were restored, the fire continued to burn with only additions of bone for about another 110 min. An effort was made to keep the fire burning efficiently and to burn the bone as completely as possible by returning fuels that fell outside of the burning area to the flames. After flames were no longer visible on the surface, the bone continued to smolder and reduce in volume for approximately another 20 min. The temperature probes were removed when the surface cooled below 150 °C and evidence for smoldering (crackling sounds and smoke) was no longer observed. This fire consumed about 4 kg of bone and 1 kg of pine wood.

Sediments were allowed to cool overnight, and the fire structure was bisected and excavated the following day. Samples of loose sediment were collected from different strata (upper white layer consisting of calcined bone), the thin black crusted layer at the top of the mineral sediment, and the lower oil saturated brownish sediment layer. A micromorphological block was taken from an intact portion of the sediment profile.

Bone Fire (EF1) Heat Profile and Duration

Figure 3 shows the temperature profile for the sediments beneath the center of the cow bone fire (EF1). The highest temperature recorded at the surface was 539 °C. At 1 cm below the surface, the high temperature was 370 °C, followed by 277 °C at 3 cm below surface, and only 91.8 °C at 5 cm below the surface. Surface temperatures over 500 °C were maintained for less than 1 h. Total burn time, with flames present, was about 3 h and 20 min.

The second peak in surface temperature shown in Fig. 3, between approximately 2:30 and 3:00, corresponds to the period when the flames were finally restored after being blown out and the remainder of the wood was consumed. Beyond this, the fire was maintained as before with only bone for another hour and 20 min. During this phase, the high temperature recorded at the surface was only 166 °C.

Unlike a wood fire, once the flame was extinguished, there were no glowing embers that could be reignited by blowing on them. An external source of open flame was required to ignite the bone fat. In this detail, a bone fire seems most similar to an oil lamp where the mineral structure of the bone serves as the vessel (and perhaps also as a wick by distributing fat in a thin layer that can be rapidly heated to flame temperature). Unlike wood, most of the structure itself does not burn and so does not form an ember or provide additional thermal energy to keep the combustion reaction going.

Field Observations During the Wood Fire (EF2)

The pine wood fire (EF2) was conducted on 25 October, 2017. The day was warm, windy, and dry. The temperature in the morning was about 24.4 °C (76 °F) and later reached 32.2 °C (90 °F). A light breeze in the morning picked up in the afternoon to about 16.1 km/h (10 mph) out of the north. Sediment moisture (measured gravimetrically) was 2.25% in the first cm and 1.53% at 5 cm below the surface.

The fire was started with splinters and shavings of pine wood and about 500 g of larger pine wood pieces. Additional wood was added as the flames began to subside. An effort was made to keep the fire burning efficiently and to burn the wood as completely as possible by returning fuels that fell outside of the burning area to the flames. The warm, dry, and windy conditions were favorable for the fire. The fire burned very efficiently and continuously with small additions of wood over a period of 3 h followed by another 2 h of coals. As the coals were consumed, the sediment cooled slowly. During the first hour, the lower coals glowed red-hot and surface temperature remained above 700 °C. Over the next hour, the coal bed was greatly diminished and temperatures eventually declined to less than 150 °C, when the probes were pulled. The experimental pine wood fire consumed approximately 5 kg of dry pine wood.

Sediments were allowed to cool and were sampled 2 days after the fire. Samples of loose sediment were collected from the upper white layer, consisting of ash and

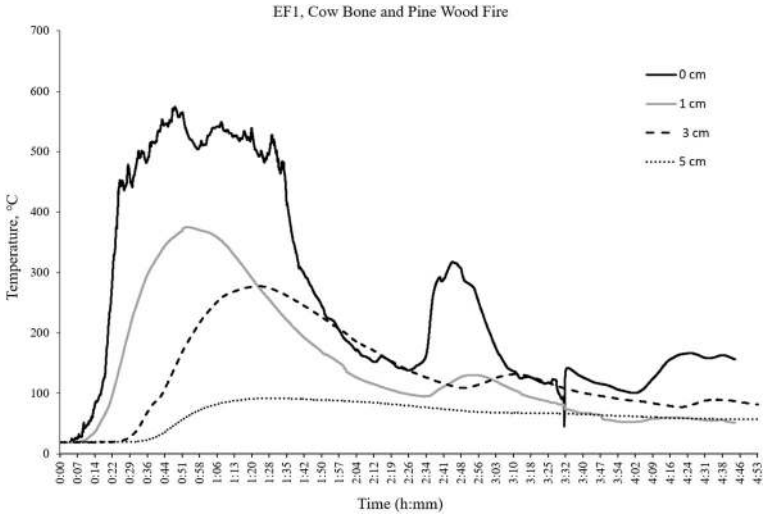

Fig. 3 Temperature profile of sediments beneath the center of the cow bone fire (EF1)

charcoal, and the thin black layer, a coating of fine black particulate matter beneath the ash layer at the top of the mineral surface. As with the bone fire, a micromorphological block was taken from an intact portion of the sediment profile.

Wood Fire (EF2) Heat Profile and Duration

Figure 4 shows the temperature profile for the sediments beneath the center of the pine wood fire. The top of the sediment reached a high temperature of 839 °C and remained above 600 °C for almost 3 h—and for large periods of that time, the temperatures climbed above 700°. One centimeter below the surface, the high temperature was 427 °C. At 5 cm, there was a delayed heat pulse that reached a maximum of 289 °C just before the surface temperature began to decline. Similar results have been obtained by other researchers after long-term heating of sediments (Aldeias *et al.* 2016). Total active burn time, where flames were present, was approximately 3 h. A seemingly anomalous feature of the temperature profile is a drop in sub-surface temperatures (1 and 3 cm below surface) that was recorded during the period of active flames when surface temperatures were at their highest (between approximately 1:35 to 2:50, Fig. 4). It is unlikely that this discrepancy was caused by changes in the location of fuels at the fire surface, as probes were stacked in a linear fashion above one another in the same portion of the fire. Interestingly, field notes also recorded an increase in wind speed at this time. Similar behavior has been noted during controlled pile-burning in an outdoor setting (M.D. Busse, personal communication, 23 August 2018). We hypothesize that strong convective conditions may have acted to pull heat upwards, resulting in a decrease in shallow sub-surface sediment temperatures.

It should be noted that the temperatures recorded in our artificial basalt sediments, below the ground surface, may be hotter than those that would be encountered under similar fire conditions in undisturbed sediments, wetter sediments, or in sediments with high organic content (Aldeias *et al.* 2016; Busse *et al.* 2010, Mallol *et al.* 2013). However, temperatures at the surface are consistent with temperatures achieved for wood fires in other contexts (Busse *et al.* 2010).

Macroscopic and Micromorphological Observations of Experimental Bone and Wood Fire Sediments

Macroscopic Observations of the Bone Fire (EF1) Footprint and Sediment Profile

After the fire was allowed to completely extinguish, a layer of fragmented calcined and charred bone remained. Little to no ash was present and a few of pieces of charcoal and unburned wood were observed. During burning, it was noted that a small amount of very fine white "gauzy" material formed as the bone was combusted. This material (bone ash?) was very fragile and was easily displaced by the wind. In agreement with prior bone burning experiments (Costamagno and Théry-Parisot 2002; Mentzer 2009, 2014; Stiner *et al.* 1995), we noted that extensive fragmentation of the bones occurred during burning. Long bones placed in the fire were originally cut into lengths between 10 and 20 cm and vertebrae were whole or halved with portions of ribs attached. The fire reduced these into much smaller pieces, ranging in size from several centimeters to sub-millimeter fragments (Fig. 5).

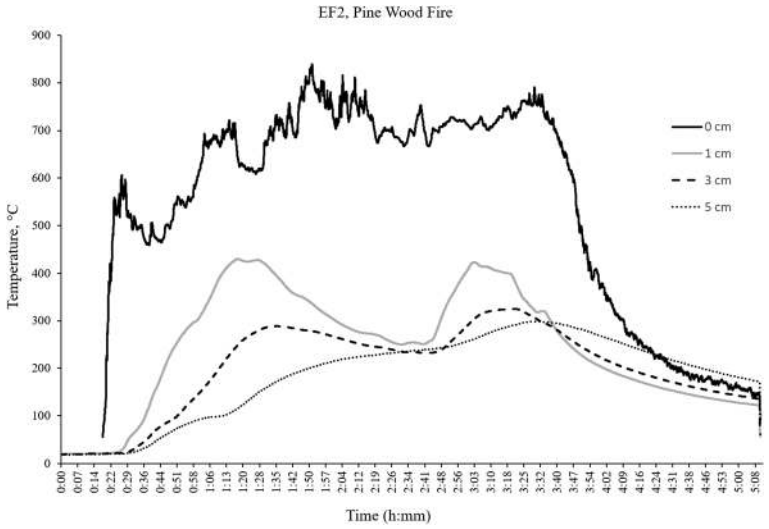

Fig. 4 Temperature profile of sediments beneath the pine wood fire (EF2)

In profile, the upper "white layer" of calcined and charred bone is several centimeters thick and rests above a crusted and tarry, asphalt-like "black layer" (Fig. 5). The blackened layer was of variable thickness and coverage on the surface. In some places, it was barely visible below the surface, in others it appeared to penetrate almost 1 cm into the sediment. Below the blackened layer is a brown fat-soaked layer where lipids penetrated to a maximum depth of approximately 4 cm into the sediment (Fig. 5). This material does not appear blackened or charred, nor does it appear reddened. Rather, it appears to be excess liquified fat that drained into the sediment before it could be heated to the point of combustion or pyrolysis. Movement of liquified fats into the sediment would have been facilitated by the heated sediments. Once the surrounding sediments became cool enough, the fats would have returned to a solid, and relatively immobile, state.

Macroscopic Observations of the Wood Fire (EF2) Footprint and Sediment Profile

The experimental pine wood fire (EF2) burned very hot and continuously in dry and windy conditions. In these favorable and highly oxic conditions, the fuel was almost entirely combusted and very little organic material appeared to remain. In profile, the uppermost layer consisted of a thin layer of ash (< 1 cm) mixed with some larger pieces of charcoal. This was underlain by a thin (1–2 mm) layer of fine black residue. Below this, the sediment was reddish brown, suggesting oxidation of the mafic substrate (Fig. 6). Unlike the primarily bone fire, the black layer was not composed of a crusted or tarry asphalt-like material and an oil-soaked brown layer was not present below the surface.

Micromorphology of the Bone Fire (EF1) Sediments

The top of the sample consists of a loose, 1–2-cm-thick layer composed exclusively of calcined bone fragments (Fig. 7). These are angular and heterometric, ranging in size

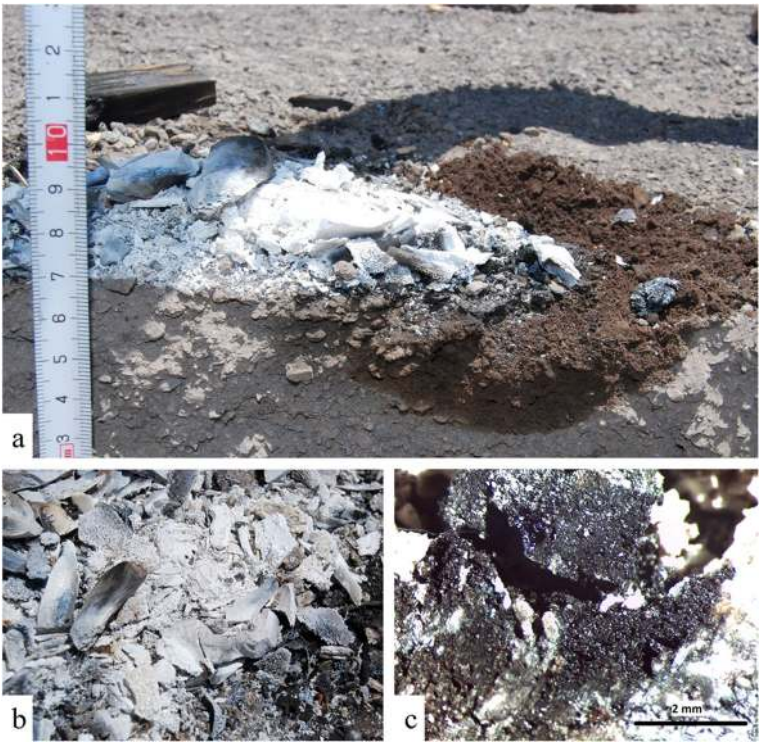

Fig. 5 Images of sediments after the bone fire. **a** The profile shows an upper "white layer" of calcined and charred bone, over a crusted, "black layer" of tarry black material in contact with the mineral surface and penetrating about 1 cm into the mineral sediment, and a lower "brown layer" where excess lipid, heated but less visibly charred, traveled several cm downward. **b** Close-up of the upper white layer showing highly fragmented calcined and charred bone. **c** Close-up view of black tarry material at contact zone in cut section (20×)

between 1 mm and several cm. A single charcoal fragment (5 mm) was observed. No char or calcareous ash were observed. Underlying this bone layer with a sharp contact is the sedimentary substrate, which is compact, horizontally fissured into 500-μm-thick lenses (Fig. 7a) and capped by a 1-mm-thick, massive black lamina across several mineral grains (Fig. 7b). The top 1 cm of the sedimentary substrate shows massive black infillings (Fig. 7c, d). Below this, no changes were observed when compared with the control substrate, which shows loose basalt grains (Fig. 8). No char, charcoal, or bone was observed in the control substrate.

Micromorphology of the Wood Fire (EF2) Sediments

The top wood ash layer was not included in the sample collected, which shows a loose mineral substrate with isolated charcoal fragments underlain by approximately 1 cm of slightly more compact microaggregated sediment composed of basalt sand grains with finer sand-sized and silt-sized black particles filling the space between them (Fig. 9). Below this segment, the matrix is compact and is similar to the control sediment. Some of the sand grains in this lower portion are rubified.

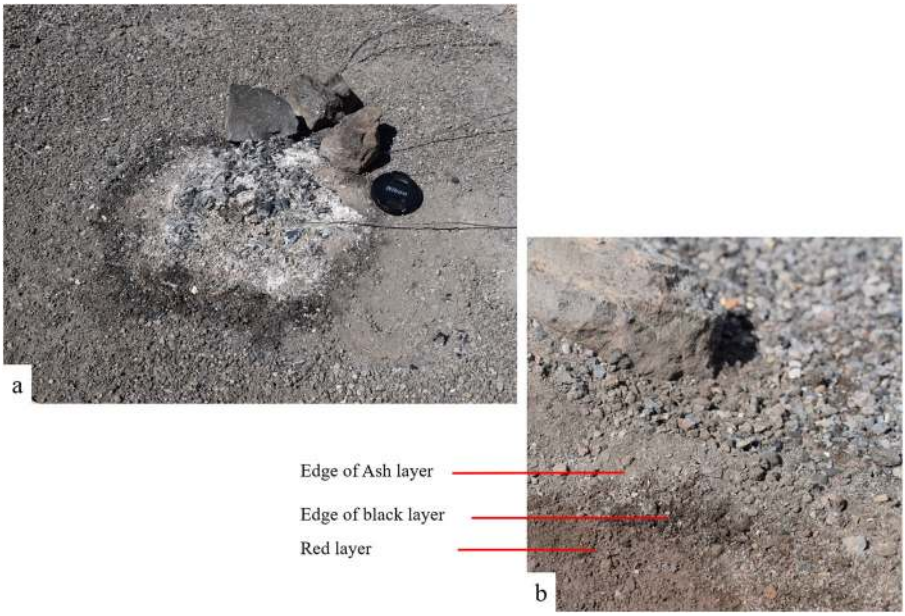

Fig. 6 Footprint (**a**) and profile (**b**) of pine wood fire after combustion. A white layer composed of ash and charcoal overlays a thin black layer of very fine black particles and a lower mineral layer which is reddened. The base of this fire, measured at the sediment surface, was hotter and remained at elevated temperatures for a longer duration than the bone fire

Molecular Data for the Bone Fire (EF1) and Cow Marrow Fat Heating Sequence

Below, the description of lipid components is broken down into the total lipid extract (TLE) and three fractions: F1, alkanes and alkenes; F2, aromatics; F3, ketones, aldehydes, long-chain esters, and nitriles (Fig. 10). Concentrations of lipids in the TLE and F1, F2, and F3 of the fire sediments are provided in Table 1. Molecular components detected in the laboratory heating series of cow marrow fat are listed and organized by fraction and TLE in Table 2. Table 3 lists the molecular components detected in layers of the experimental cow bone fire (EF1), and the experimental pine wood fire (EF2). It should be noted that F1, F2, and F3 were not derivatized and so the methyl esters listed in F3 are a result of pyrolysis. This contrasts with the methyl esters reported in the TLE. Because the TLE is dominated by fatty acids, which are more polar than the compounds present in F1, F2, and F3, derivatization was necessary to facilitate analysis *via* GC/MS and GC/IRMS. As a consequence of derivatization, free fatty acids as well as fatty acids remaining as tri-, di-, or mono-acyl glycerides were trans-esterified to fatty acid-methyl esters (FAMES).

The presence of certain types of lipid compounds listed below (alkanes and alkenes, aromatics, nitriles, long-chain esters, and long-chain ketones) in heated cow fat can be attributed to pyrolysis (Fig. 10). These molecules were not detected in the unheated cow marrow fat, or the basalt sediment. Instead, they appeared in cow marrow fat residues after experimental heating in the muffle furnace at temperatures of 300 °C, 350 °C, and 400 °C (Table 2, Fig. 12). The formation of many of these products has also been described during thermal processing of animal fats and plant oils (Ayllón *et al*. 2006; Ben Hassen-Trabelsi

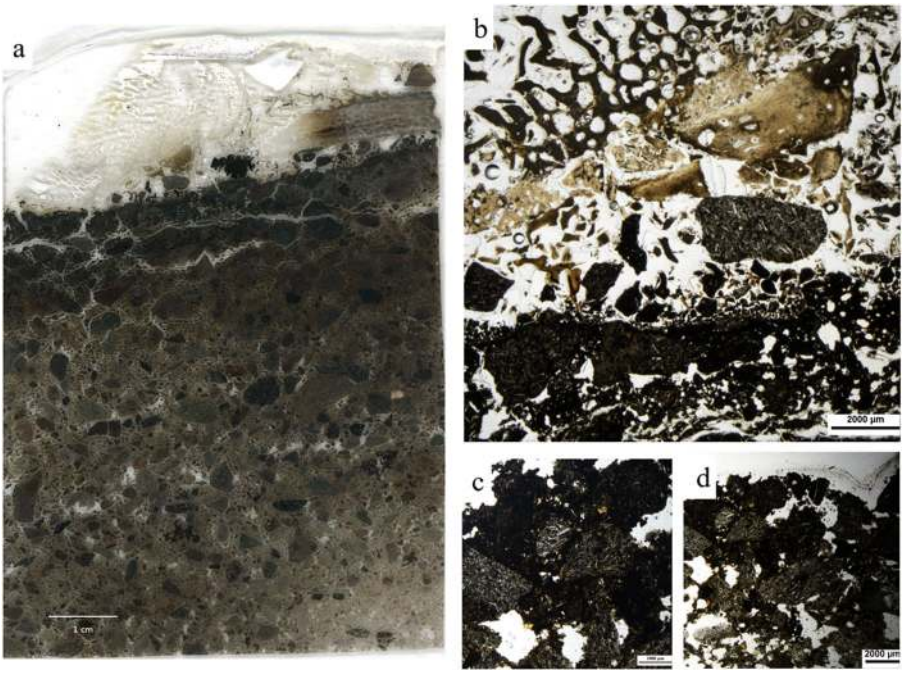

Fig. 7 Experimental bone fire (EF1) sediment. **a** Flatbed scan image of the thin section. **b–d** Microphotographs taken in plane-polarized light. **b** The basalt sand substrate (dark gray) with amorphous black matter coating the grains and partially infilling the space between them. Overlying the basalt substrate is an accumulation of highly fragmented, calcined, and strongly burnt bone. **c**, **d** Detail of dark amorphous material coating basalt grains and infilling spaces

et al. 2014; Chaiwong *et al*. 2013; Kim *et al*. 2014; Ma and Hanna 1999; Maher and Bressler 2007, Maher *et al*. 2008; Nawar 1969; Schwab *et al*. 1988). Lipid residues in our 400 °C treatment were very low, however, probably due to the presence of oxygen during heating. Although the crucibles were covered with foil, they were not air-tight, and we suspect that at 400 °C, most of the heated material was lost due to volatization and combustion. The low amount of lipids including pyrolysis products is related to the presence of oxygen at high temperatures, rather than the high temperatures alone. In the absence or near absence of oxygen (conditions favorable for pyrolysis rather than combustion), higher yields of products such as long-chain ketones and alkanes are, in fact, routinely reported for temperatures above 400 °C versus lower temperatures (Ben Hassen-Trabelsi *et al*. 2014; Raven *et al*. 1997; Schwab *et al*. 1988).

Total Lipid Extract

The TLE of the brown and black layers of the cow bone fire (EF1) contained more than a milligram of lipid per gram of sediment, with fatty acids comprising by far the greatest portion of all lipids (Table 1). The total lipid extract in the white layer (primarily calcined bone) contained a much lower lipid concentration than the lower layers, approximately 14 μg/g of calcined bone. Also, the concentration of the TLE for all layers of the cow bone fire was approximately two to four orders of magnitude

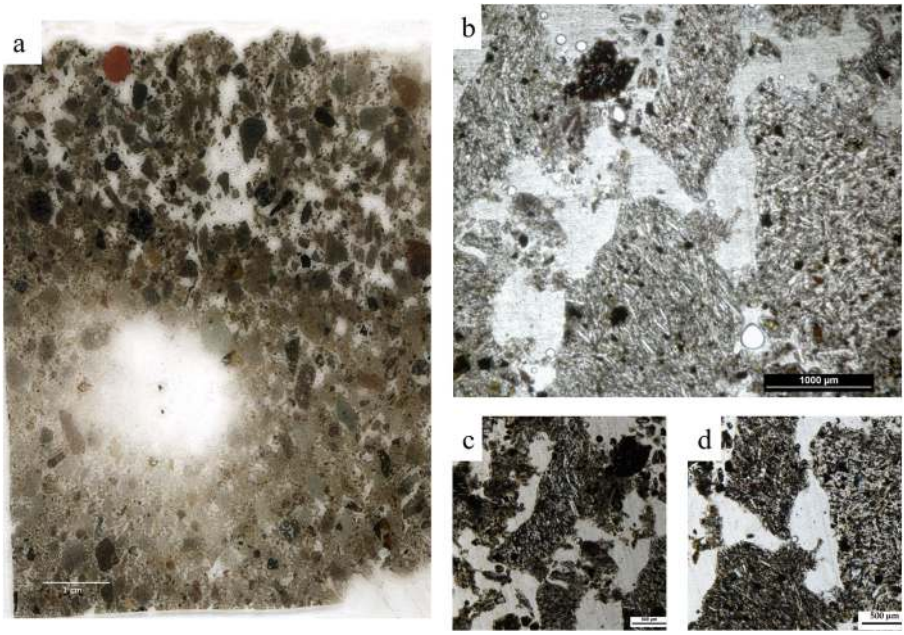

Fig. 8 Control sediment for experimental fires. **a** Flatbed scan image of the thin section. The top part is loose and compact below 2–3 cm. The white circle is empty space resulting from thin section manufacture. **b–d** Microphotographs taken in plane-polarized light. Prior to input from fires, the control sediment shows a loose, vughy microstructure. It is composed of angular basalt sand. The individual grains do not show any kind of coating of fine matter between them

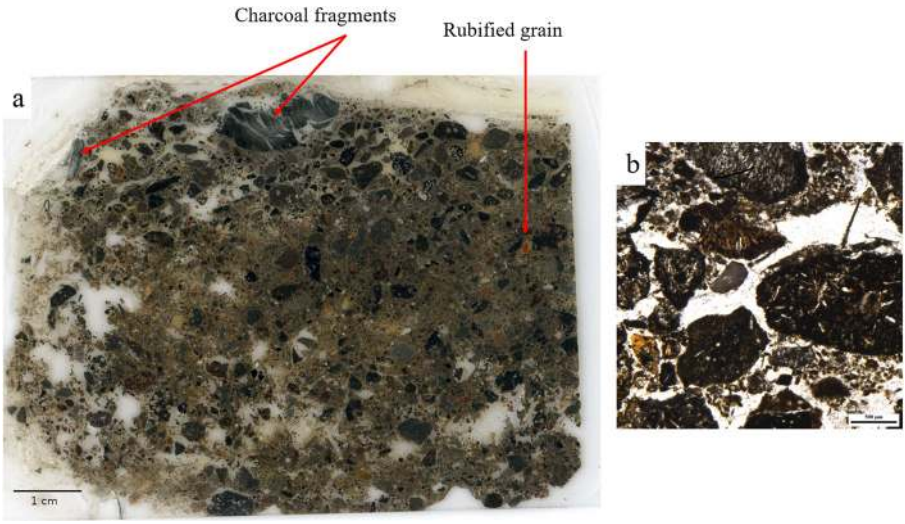

Fig. 9 Experimental wood fire (EF2) sediment. **a** Flatbed scan image of the thin section. The top wood ash layer is not present in the sample, which shows a loose mineral substrate with isolated charcoal fragments underlain by a compact, basalt sand matrix similar to the control sediment. Some of the sand grains in this lower portion are rubified. **b** Microphotograph representative of the sediment below the charcoal fragments (up to 1 cm below) taken in plane-polarized light. The basalt sand shows an intergrain microaggregate structure with finer sand-sized and silt-sized black particles filling the space between larger basalt grains

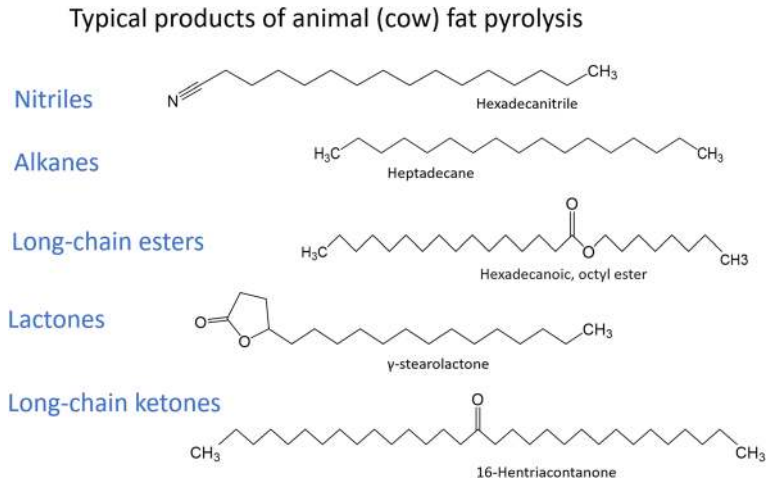

Fig. 10 Examples of aliphatic products of pyrolyzed animal fat

greater than the concentration of lipids in their corresponding molecular fractions. The concentration of lipids in F1, F2, and F3 ranged between 5.71 and 0.01 micrograms of lipid per gram of sediment (Table 1).

The TLE of the black layer of the cow bone fire contained the same types of compounds that were present in the cow marrow fat heating experiments at 300 °C and 350 °C, plus several of the most abundant pyrolysis products observed in the fractions (Tables 2 and 3). This included saturated *n*-chain fatty acids from 12 to 20 carbons in length, with a maximum at 16 and 18 carbons (hexadecenoic and octadecanoic acids) and the next largest peak at 14 carbons (tetradecanoic acid). Branched-chain, saturated fatty acids (anteiso and iso) 15 and 17 carbons in length were also present in lower amounts. Monounsaturated fatty acids included those with 14, 16, 17, and 18 carbon chains. Several $C_{18:1}$ isomers were also present in the brown and black layers, but preservation of the monounsaturated fats was highest in the brown layer. This is visible by comparison of the $C_{18:1}$ to the $C_{18:0}$ peaks in Fig. 11.

Oxidation products present in the TLE included saturated dicarboxylic acids from 7 to 11 carbons in length, and two isomers of 9,10-dihydroxy-octadecanoic acid (see Passi *et al.* 1993; Hansel and Evershed 2009). A few pyrolysis products (several nitriles and γ-stearolactone) were also detected in the TLE of the black layer. That more pyrolysis products were not detected in the TLE, but are clearly present in the fractions, is probably due to significant peak overlap and the low relative abundance of many pyrolysis products compared to the fatty acids. Due to the very large difference in concentration (in some cases more than 1000:1) and the partial or total overlap of some of these molecules by fatty acid peaks, it would have been difficult or impossible to determine the contribution of specific alkanes, aromatics, and ketones by GC/MS without prior separation.

Alkanes (F1)

Black and brown layers from the cow bone fire (EF1) contained a series of short-chain *n*-alkanes and *n*-alkenes, with a maximum at C_{17} (heptadecene and heptadecane)

Table 2 Molecular components of the cow bone fat laboratory furnace heating series

Sample	F1 alkanes	F2 aromatics	F3 ketones, aldehydes, nitriles, long-chain esters	TLE with FAME derivatization[a]
Basalt sediment	No measurable *n*-alkanes	No measurable aromatics	No measurable ketones, aldehydes, nitriles, or long-chain esters	No measurable components
Cow marrow fat, unheated	No measurable *n*-alkanes	No measurable aromatics	No measurable ketones, aldehydes, nitriles, or long-chain esters	Saturated fatty acids ($C_{14:0}$, $C_{15:0}$, *$C_{16:0}$*[b], $C_{17:0}$, *$C_{18:0}$*); monounsaturated fatty acid ($C_{14:1}$, *$C_{16:1}$ isomers*, $C_{17:1}$, *$C_{18:1}$ isomers*, $C_{20:1}$); polyunsaturated fatty acid ($C_{18:2}$ isomers), branched-chain saturated fatty acids (C_{15}, C_{17}) squalene, cholesterol
Cow marrow fat + basalt sediment 300 °C	*n*-Alkanes (C_{15}, C_{16}, *C_{17}*) *n*-alkenes (C_{15}, *C_{17}*), cyclohexadecane, undecylcyclohexane	*Undecylbenzene*, other alky substituted benzenes, alkyl substituted naphthalene, other aromatics	Tetradecanitrile, pentadecanitrile, *hexadecanitrile*, *oleanitrile*, *octadecanitrile*, tetradecanoic acid-methyl ester, hexadecanoic acid-methyl ester, tetradecenoic acid-butyl ester, hexadecanoic acid-ethyl ester, hexadecanoic acid-propyl ester, 9-octadecenoic acid-methyl ester,11-octadecenoic acid-methyl ester, 10-octadecenoic acid-methyl ester, octadecanoic acid-methyl ester, 9-octadecenoic acid-ethyl ester, tetradecanoic acid-hexyl ester, hexadecanoic acid-butyl ester, octadecanoic acid-ethyl ester, trans-9-octadecenoic acid-pentyl ester, cis-9-octadecenoic acid-propyl ester, hexadecanoic acid-pentyl ester, octadecanoic acid-propyl ester, trans-9-octadecenoic acid-pentyl ester, trans-9-octadecenoic acid-pentyl ester, hexadecanoic acid-hexyl ester, octadecanoic acid-butyl ester, trans-9-octadecenoic acid-pentyl ester, trans-9-octadecenoic acid-pentyl ester, hexadecanoic acid-heptyl ester, octadecanoic acid-pentyl ester, trans-9-octadecenoic acid-pentyl ester, trans-9-octadecenoic acid-pentyl ester, hexadecanoic acid-octyl ester, octadecanoic acid-hexyl ester, trans-9-octadecenoic acid-pentyl ester; 16-hentriacontanone (trace amount)	Dicarboxylic fatty acids ($C_{7–11}$), saturated fatty acids (*$C_{14:0}$*, $C_{15:0}$, *$C_{16:0}$*, $C_{17:0}$, *$C_{18:0}$*), monounsaturated fatty acids ($C_{14:1}$, $C_{16:1}$ isomers, $C_{17:1}$, *$C_{18:1}$ isomers*, $C_{20:1}$), branched-chain saturated fatty acids (C_{15} and C_{17}), 9,10-dihydroxy-octadecanoic acid

Table 2 (continued)

Sample	F1 alkanes	F2 aromatics	F3 ketones, aldehydes, nitriles, long-chain esters	TLE with FAME derivatization[a]
Cow marrow fat + basalt sediment 350 °C	*n*-Alkanes (C_{15}, C_{16}, *C_{17}*) *n*-alkenes (C_{15}, *C_{17}*), cyclohexadecane, undecylcyclohexane	*Undecylbenzene*, dodecylbenzene, other alky substituted benzenes, alkyl substituted naphthalenes, other aromatics	Saturated *n*-aldehydes (C_{12}, C_{13}, C_{14}, C_{15}, C_{16}), 2-pentadecanone, tetradecanitrile, pentadecanitrile, *hexadecanitrile*, *oleanitrile*, *octadecanenitrile*, tetradecanoic acid-methyl ester, hexadecanoic acid-methyl ester, hexadecanoic acid-ethyl ester, octadecenoic acid-methyl ester, octadecanoic acid-methyl ester, hexadecanoic acid-butyl ester, octadecanoic acid-ethyl ester, octadecenoic acid-propyl ester, hexadecanoic acid-pentyl ester, octadecanoic acid-propyl ester, hexadecanoic acid-hexyl ester, octadecanoic acid-butyl ester, hexadecanoic acid-heptyl ester, octadecanoic acid-pentyl ester, hexadecanoic acid-octyl ester, octadecanoic acid-hexyl ester, octadecanoic acid-heptyl ester, octadecanoic acid-octyl ester, 14-nonacosanone, 16--hentriacontanone, 16-tritriacontanone, 18-pentatriacontanone	Saturated fatty acids ($C_{14:0}$, $C_{15:0}$, *$C_{16:0}$*, $C_{17:0}$, *$C_{18:0}$*); monounsaturated fatty acids ($C_{16:1}$, $C_{17:1}$, *$C_{18:1}$ isomers*), branched-chain saturated fatty acids (C_{17}), 4-hydroxy-octadecanoic acid
Cow marrow fat + basalt sediment 400 °C	*n*-Alkanes in trace amounts	No measurable aromatics	No measurable ketones, aldehydes, nitriles or long-chain esters	Saturated fatty acid-methyl esters ($C_{16:0}$, $C_{18:0}$)

[a] All fatty acids shown were fatty acid-methyl ester derivatives, and dicarboxylic acids were dimethyl ester derivatives

[b] Major peaks are in italic font

(Table 3). Figure 12 compares the TICs for the alkane fraction (F1) of the cow marrow fat heating series. No alkanes are present in fresh cow marrow fat. At 300 °C, short-chain alkanes and alkenes are present, dominated by heptadecene and heptadecane. At 350 °C, the concentration of heptadecene and heptadecane increases further. At 400 °C, trace amounts of alkanes were present, but as described above, much of the material was probably lost as volatilized or combusted material. With the exception of trace amounts of heptadecane, no other alkane or alkene components were detected in F1 of the white layer.

The short-chain *n*-alkanes and *n*-alkenes, maximizing at C_{17} in the brown and black layers, most likely formed from pyrolysis of some of the most abundant fatty acids, $C_{18:1}$ isomers and $C_{18:0}$, in cow marrow fats. Several studies of the pyrolysis of cow fats for biofuels also show the formation of short-chain alkanes with a maximum at C_{17} (Ben Hassen-Trabelsi *et al.* 2014; Maher *et al.* 2008). Thermal generation of short-chain *n*-alkanes and *n*-alkenes occurs through a loss of CO_2 from precursor fatty acids at temperatures above 300 °C (Chang and Wan 1947; Maher and Bressler 2007; Maher *et al.* 2008; Schwab *et al.* 1988; Srivastava and Prasad 2000). The thermal decomposition of saturated and unsaturated fatty acids to *n*-alkanes and *n*-alkenes occurs through the following reaction:

$$RCOOH \underset{High\ \ Temp}{\rightarrow} RH + CO_2$$

This reaction may proceed through a $RCOO^{\bullet}$ radical formed during triglyceride cleavage, followed by a loss of CO_2 (Maher and Bressler 2007; Maher *et al.* 2008; Schwab *et al.* 1988). The loss of CO_2 results in *n*-alkanes and *n*-alkenes that are one carbon shorter than precursor molecules.

Aromatics (F2)

Very low amounts of aromatics were detected in the black and brown layers of the cow bone fire and in the muffle furnace heating experiments with cow marrow fat (Table 1). These consisted of alkyl substituted benzenes (undecyl benzene and dodecyl benzene, in particular) as well as alkyl substituted naphthalene (Tables 2 and 3). One mechanism for the formation of these aromatic compounds may be through Diels-Alder reactions involving unsaturated fatty acids. Schwab *et al.* (1988:85) suggest that aromatics form during pyrolysis of fats "through a Diels-Alder addition of ethylene to a conjugated diene."

Ketones, Esters, and Nitriles (F3)

Similar to what has been demonstrated in experimental and archaeological pottery (Evershed *et al.* 2002a; Raven *et al.* 1997), a series of saturated long-chain symmetrical and slightly asymmetrical ketones (14-nonacosanone, 16-hentriacontanone, 16-tritriacontaneone, and 18-pentatriacontaneone) formed in the black layer of the experimental cow bone fire from precursor fatty acids (Fig. 13). These same ketones were also formed in the muffle furnace experiments at 350 °C, and to a lesser extent at 300 °C, but were not present in unheated cow marrow fat. Previous studies have shown that these molecules form at elevated temperatures through ketonic decarboxylation of

Table 3 Molecular components of layers of the cow bone fire (EF1) and the wood fire (EF2)

Sample	F1 alkanes	F2 aromatics	F3 ketones, aldehydes, nitriles, esters	TLE with FAME derivatization[a]
EF1 white	Trace amount of *n*-alkane C_{17}	No measurable aromatics	2-Pentadecanone, *hexadecanitrile*[b], *oleanitrile*, *octadecanenitrile*, hexadecanoic acid-methyl ester	Dicarboxylic acids ($C_{9–11}$), saturated fatty acids ($C_{12:0}$, $C_{14:0}$, $C1_{5:0}$, *$C_{16:0}$*, $C_{17:0}$, *$C_{18:0}$*), monounsaturated fatty acids ($C_{14:1}$, $C_{16:1}$ isomers, $C_{17:1}$, $C_{18:1}$ isomers, $C_{20:1}$), polyunsaturated fatty acids ($C_{18:2}$), branched-chain saturated fatty acids (C_{15} and C_{17}), hexadecanitrile, oleanitrile, octadecanenitrile
EF1 black	*n*-Alkanes (C_{15}, C_{16}, *C_{17}*) *n*-alkenes (C_{15}, *C_{17}*), cyclohexadecane, undecylcyclohexane	*Undecylbenzene*, decylbenzene, other alkyl substituted benzenes, alkyl substituted naphthalenes	Saturated *n*-aldehydes (C_{11},C_{12}, C_{13}, C_{14}, C_{15}, C_{16}, C_{17}), tetradecanitrile, 11-pentadecenal, 2-pentadecanone, 9-hexadecenal, *hexadecanenitrile*, *oleanitrile*, *octadecanenitrile*, hexadecanoic acid-methyl ester, octadecanoic acid-methyl ester, hexadecanoic acid-pentyl ester, 9-octadecenoic acid-butyl ester, hexadecanoic acid-hexyl ester, 9-octadecenoic acid-pentyl ester, hexadecanoic acid-heptyl ester, 9-octadecenoic acid-hexyl ester, hexadecanoic acid-octyl ester, octadecanoic acid-hexyl ester, octadecanoic acid-heptyl ester, octadecanoic acid-octyl ester, 14--nonacosanone, 16-hentriacontanone, 16--tritriacontanone, 18-pentratriacontanone	Dicarboxylic acids ($C_{7–11}$), heptadecane, saturated fatty acids ($C_{12:0}$, $C_{13:0}$, *$C_{14:0}$*, $C_{15:0}$, *$C_{16:0}$*, $C_{17:0}$, *$C_{18:0}$*), monounsaturated fatty acids ($C_{14:1}$, $C_{16:1}$ isomers, $C_{17:1}$, *$C_{18:1}$ isomers*, $C_{20:1}$), polyunsaturated fatty acids ($C_{18:2}$), branched-chain saturated fatty acids (C_{15} and C_{17}), hexadecanitrile, oleanitrile, octadecanenitrile, γ-stearolactone, 3-octyl-oxiraneoctanoic acid-methyl ester, 9,10-dihydroxy-octadecanoic acid-methyl ester (2 isomers)
EF1 brown	*n*-Alkane *C_{17}*, *n*-alkene *C_{17}*	Trace amounts of phenanthrene, pyrene, retene, and other aromatics	Saturated *n*-aldehydes (C_{14}, C_{15}, C_{16}), *hexadecanitrile*, *oleanitrile*, *octadecanitrile*, hexadecanoic acid-methyl ester, 16-hentriacontanone (trace amount)	Dicarboxylic acid (C_9), saturated fatty acids ($C_{12:0}$, $C_{13:0}$, *$C_{14:0}$*, $C_{15:0}$, *$C_{16:0}$*, $C_{17:0}$, *$C_{18:0}$*), monounsaturated fatty acids ($C_{14:1}$, $C_{16:1}$ isomers, $C_{17:1}$, *$C_{18:1}$ isomers*, $C_{20:1}$), polyunsaturated fatty acids ($C_{18:2}$), branched-chain saturated fatty acids (C_{15} and C_{17}), 3-octyl-oxiraneoctanoic acid-methyl ester, 9,10-dihydroxy-octadecanoic acid-methyl ester

Table 3 (continued)

Sample	F1 alkanes	F2 aromatics	F3 ketones, aldehydes, nitriles, esters	TLE with FAME derivatization[a]
EF2 white	No measurable alkanes	No measurable aromatics	No measurable ketones, aldehydes, nitriles, or long-chain esters	Saturated fatty acids (*$C_{16:0}$*, *$C_{18:0}$*), monounsaturated fatty acids ($C_{18:1}$, $C_{22:1}$), methyl dehydroabietate, stigmasten-3,5-diene
EF2 black	Trace amounts of alkanes	No measurable aromatics	No measurable ketones, aldehydes, nitriles, or long-chain esters	Saturated fatty acids ($C_{12:0}$, $C_{14:0}$, $C_{15:0}$, $C_{16:0}$, $C_{18:0}$), monounsaturated fatty acids ($C_{16:1}$, $C_{18:1}$, $C_{22:1}$), saturated fatty acid-ethyl esters (*$C_{16:0}$*, *$C_{18:0}$*), methyl dehydroabietate, stigmasten-3,5-diene

[a] All fatty acids shown were fatty acid-methyl ester derivatives, and dicarboxylic acids were dimethyl ester derivatives

[b] Major peaks are in italic font

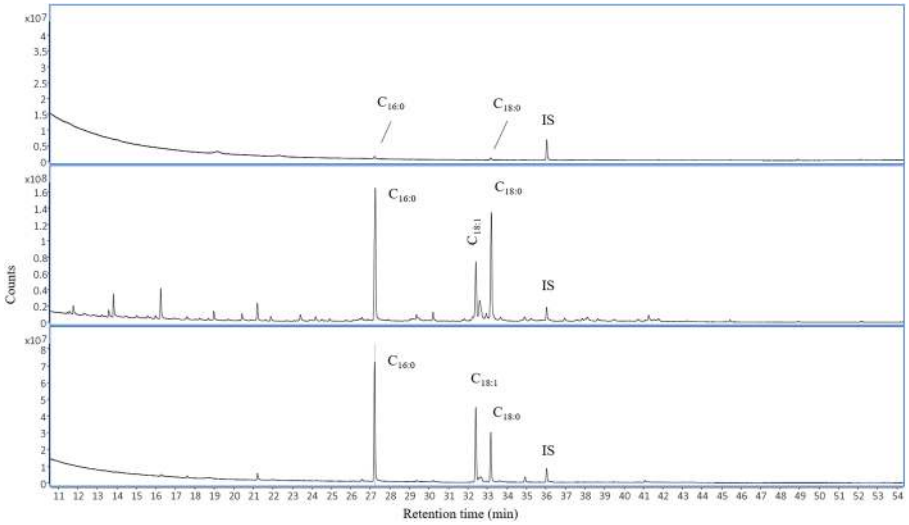

Fig. 11 Total ion chromatograms of F5 FAMES for white (upper), black (middle), and brown (lower) layers of the experimental cow bone fire. The largest amount of lipid is in the black layer. The black layer also contains the greatest variety of pyrolysis products. The brown layer appears to be the least affected by heat as fewer pyrolysis products are present and, like fresh cow fat, there is a greater proportion of the unsaturated fatty acid $C_{18:1}$ to $C_{18:0}$

the free form of stearic and palmitic fatty acids as well as from the triglycerides tripalmitin and tristearin (Raven *et al*. 1997; Renz 2005). Ketonic decarboxylation takes place *via* the following reaction:

$$R^1COOH + R^2COOH \underset{>300^\circ C}{\rightarrow} R^1COR^2 + CO_2 + H_2O$$

Ketonic decarboxylation may occur through a free radical mechanism at elevated temperatures (Renz 2005; Pham *et al*. 2013) or following basic adduction of a hydrogen from an alpha carbon (the carbon adjacent to the carbonyl group) (Pham *et al*. 2013). The latter mechanism seems to be especially important for surface-catalyzed ketonization (Pham *et al*. 2013) and is shown in Fig. 14. The presence of fired clay matrix and divalent metal oxides have been shown to substantially increase product yields, separately, and in concert (Raven *et al*. 1997). This is consistent with current understandings of ketonization mechanisms which suggest that that two different processes, bulk ketonization and surface-catalyzed ketonization, can occur together or separately depending on thermal conditions and the presence of different catalyzing agents (Pham *et al*. 2013; Renz 2005).

Palmitic ($C_{16:0}$) and stearic ($C_{18:0}$) acids are (respectively) the first and second most abundant saturated fatty acids in cow marrow fat, and ketonic decarboxylation of these precursors results in the following combination of long-chain symmetrical and asymmetrical ketones: 16-hentriacontanone, 16-tritriacontanone, and 18-pentatriacontanone). The 31-carbon symmetrical ketone, 16-hentriacontanone (31 K), is formed from two palmitic acids; a slightly asymmetric 33 carbon ketone, 16-tritriacontanone (33 K), is formed from the combination of one palmitic and one stearic

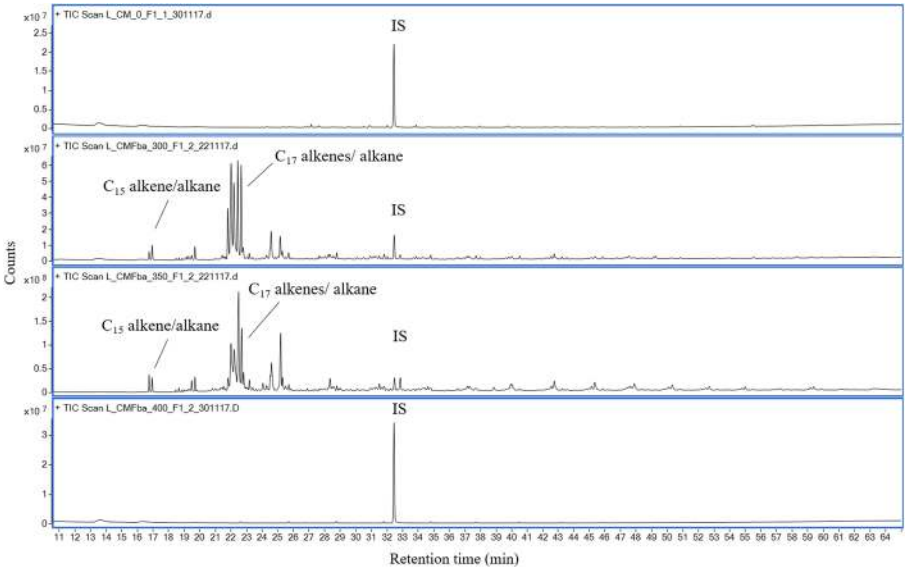

Fig. 12 Total ion chromatograms of alkenes and alkanes in F1 from a cow marrow fat heating series. At the top is unheated cow marrow fat, followed by cow marrow fat heated to 300 °C, 350 °C, or 400 °C for 60 min. No *n*-alkenes or *n*-alkanes were detected in unheated marrow fat. At 300 °C and 350 °C, C_{15} and C_{17} *n*-alkene and *n*-alkane peaks are present. Several peaks representing different C_{17} *n*-alkene isomers are present. This is consistent with the presence of several $C_{18:1}$ fatty acid isomers (probable precursor molecules) that are found in unheated cow marrow fat. At 400 °C, only trace amounts of *n*-alkanes were detected

acid; and 18-pentatriacontanone, a symmetric 35-carbon ketone (35 K), is formed from two stearic acids. The third most prevalent saturated fatty acid in cow fat is myristic acid ($C_{14:0}$). Accordingly, a low amount of 14-nonacosanone, a 29-carbon slightly asymmetric fatty acid (29 K), was also identified in the black layer and muffle furnace experiments with cow marrow fat. This molecule is the expected product of ketonic decarboxylation of palmitic acid ($C_{16:0}$) and myristic acid ($C_{14:0}$).

The long-chain ketones were best represented in the black layer of the cow bone fire and in the sample of cow marrow fat that was heated to 350 °C. Only one symmetric long-chain ketone (16-hentriacontanone) was detected in the brown layer of the cow bone fire, and no ketones were detected in the white layer (calcined bone). The lack of ketones and generally low amount of lipids in the white layer was not unexpected. Calcination occurs at high temperatures in the presence of oxygen rather than under anoxic conditions (Reidsma *et al*. 2016) and results in a very white matrix with little to no measurable organic content (Munro *et al*. 2007; Snoeck *et al*. 2014; Stiner *et al*. 1995).

An important caveat, with potential significance for identifying multiple heating events in combustion features, comes from reheating previously calcined bone with fresh cow marrow fat. We performed a reheating experiment by adding fresh cow marrow fat to previously calcined bone and heating them together in the muffle furnace at 350 °C for 60 min. This produced a very high concentration of long-chain symmetrical and slightly asymmetrical ketones. In fact, the amount formed with calcined bone was orders of magnitude greater than the amount produced under similar conditions with the crushed basalt sediment (Fig. 15). Given the same proportions of starting materials (fat to matrix, 1:10 wt/wt), at 350 °C, the basalt matrix produced less than

15 μg per g of crushed basalt, while the bone matrix produced approximately 800 μg of long-chain ketones per g of crushed calcined bone.

Although the initial process of calcination destroys nearly all organic content, previously calcined bone appears to be an excellent medium for the production of long-chain symmetrical and slightly asymmetrical ketones from newly introduced animal fat. It has very high porosity and surface area, and basic sites in the mineral surface of calcined bone should promote surface-catalyzed ketonization. Calcined bone loses structural carbonate and reorganizes phosphate and calcium (Munro *et al.* 2007; Reidsma *et al.* 2016; Stiner *et al.* 1995). Some studies have noted the formation of small amounts of tricalcium phosphate and/or calcium oxide (Munro *et al.* 2007; Stiner *et al.* 1995). Calcium oxide, in particular has previously been identified as a highly effective catalyst in the formation of long-chain ketones from fats (Pham *et al.* 2013; Raven et al. 1997; Renz 2005). Given these structural and chemical changes, surface-catalyzed ketonization (Pham *et al.* 2013) may play a large role in the formation of symmetrical ketones where heated fat is in contact with previously calcined bone.

These observations need to be replicated, but could be very significant for identifying the presence of more than one burning event in archaeological contexts. In particular, because calcined bone can initially be expected to contain very little original lipid material, the presence of abundant fats in calcined bones may aid in recognizing and analyzing input from sequential episodes of burning.

In addition to these saturated symmetric and slightly asymmetric long-chain ketones, 2-pentadecanone (a methyl-ketone) was also detected in the black layer and cow fat heated to 350 °C (Tables 2 and 3). Methyl-ketones have been noted in the thermal production of biofuel and are believed to form through a more complex pathway than the symmetrical long-chain ketones discussed above (Nawar 1969; Schwab *et al.* 1988). Due to the position of the reactive carbonyl group at the end of these molecules, methyl-ketones are more susceptible to degradation than saturated symmetric and

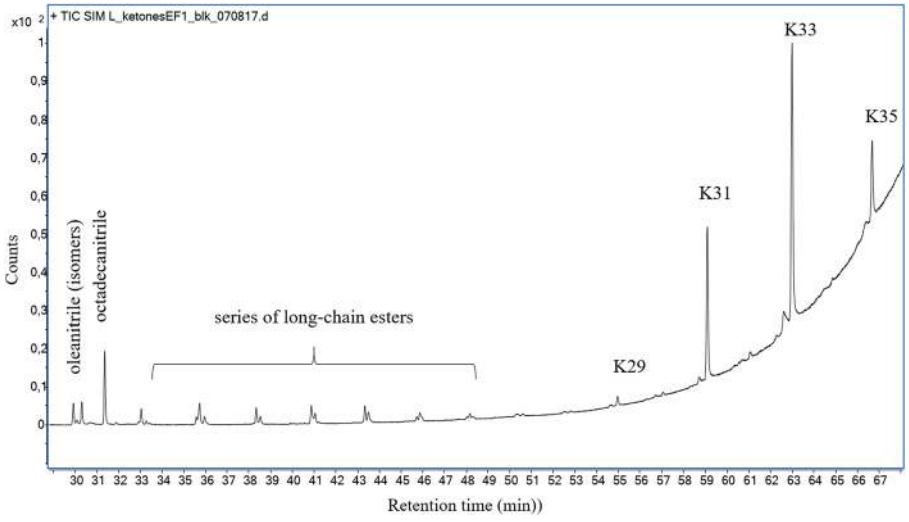

Fig. 13 Partial TIC for F3 of the experimental bone fire showing a series of long-chain symmetrical and asymmetrical ketones 14-nonacontanone (K29), 16-hentriacontanone (K31), 16-tritriaconanone (K33), and 18-pentatriacontanone (K35)

slightly asymmetric long-chain ketones. Short-chain methyl ketones like 2-pentadecanone are also fairly volatile (decreasing their residence time in sediments) and are produced by some fungi and insects (Forney and Markovetz 1971). For these reasons, we do not consider short-chain methyl-ketones to be strong candidates for archaeological biomarkers of animal fats. Nevertheless, 2-pentadecanone and 2-heptadecanone have been identified in several experimental and archaeological studies of burned animal fats (Lejay *et al.* 2016; March and Lucquin 2006; Lucquin 2007) and their presence in comparison to controls could prove useful as supplementary indicators of animal fat pyrolysis.

Some of the largest peaks in F3 of the black and the brown layers of the cow bone fire and the experimentally heated cow fat are a series of saturated and monounsaturated nitriles with a maximum at C_{16} and C_{18} (hexadecanitrile, oleanitrile, and octadecanitrile) (Tables 2 and 3, Fig. 10). The nitriles are produced by reactions between fatty acids and amino acids from endogenous proteins. These aliphatic nitrogen-containing compounds are among the most prevalent compounds documented in the pyrolysis of meat and bone meal (Ayllón *et al.* 2006) and also form as byproducts during the synthesis of biofuels (Ben Hassen-Trabelsi *et al.* 2014:216; Chaiwong *et al.* 2013). Unfortunately, nitriles are likely to be more susceptible to degradation than long-chain symmetrical ketones or alkanes. The reactivity of nitriles is similar to that of carboxylic acids because the cyano group at the end of the carbon chain is strongly polarized (McMurry 1992:824–828).

Finally, a homologous series of long-chain esters are present in F3 of the black layer and the brown layer of the experimental bone fire as well as in experimentally heated cow marrow fat (Tables 2 and 3, Fig. 10). The ester components decreased in concentration as the heating temperature increased from 300 to 350 °C. At the same time, ketones increased and a number of aldehydes appeared in cow fat heated to 350 °C. The ester bond in these molecules makes them more reactive and less likely to survive archaeological time than saturated long-chain symmetrical ketones or alkanes (Cranwell 1981).

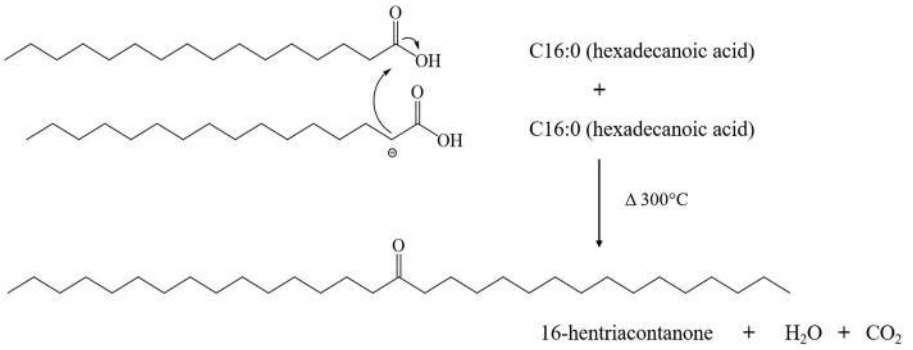

C14:0 + C16:0 = K29	14-nonacosanone
C16:0 + C16:0 = K31	16-hentriacontanone
C18:0 + C16:0 = K33	16-tritriacontanone
C18:0 + C18:0 = K35	18-pentatriacontanone

Fig. 14 Mechanism of ketonic decarboxylation following removal of an α-hydrogen by a basic site on the surface of a solid catalyst (Pham *et al.* 2013)

Molecular Data for the Wood Fire (EF2)

As detailed above, the wood fire burned quite hot and the fuel was almost entirely consumed. With very high temperatures and highly oxic conditions, combustion and not pyrolysis is expected to prevail. Under conditions of efficient combustion, nearly all of the organic fuels should be converted to atmospheric carbon. Indeed, very little organic material remained to be extracted. The concentration of fatty acids present in the black layer of the wood fire is much lower than in the bone fire. The total lipid extract in the black layer of the wood fire is less than half a microgram of lipid per gram of sediment, while the TLE of the bone fire contained more than a milligram per gram of lipid per gram of sediment (Table 1). As with the bone fire, concentrations of extractable lipids were lower in the white layer compared to the black layer. Unfortunately, a sample of the reddened layer was not collected and the organic content of this layer was not analyzed. Due to the very low amounts of lipid detected in the black layer, however, it is unlikely that the reddened layer contained more lipid than was present in the control sediment, which was essentially blank (Table 2).

Overall, the white and black layers of the pine wood fire contained few lipids (Table 3). Saturated fatty acids between 12 and 18 carbons long, and low amounts of monounsaturated fatty acids 16, 18, and 22 carbons long, were present in the black layer. The TLE of the black layer also contained low amounts of ethyl esters of hexadecanoic and octadecanoic acids (products of pyrolysis), as well as methyl dehydroabietate and stigmasten-3,5-diene. Lipid components detected in the white layer were limited to saturated fatty acids. Total amounts of lipids in F1, F2, and F3, for both the white and black layer samples, were too low to detect (Tables 1 and 3).

Summary of Molecular Data for the Bone Fire (EF1), Cow Marrow Fat Heating Series, and Wood Fire (EF2)

White, black, and brown layers (described above) of the experimental bone fire contained a number of the same molecules, but many components detected in the black layer were not found in the white or brown layers. The TLE and all fractions of the black layer contained the highest concentration of lipids and the greatest number of components. The lowest concentration and fewest components were detected in the white layer.

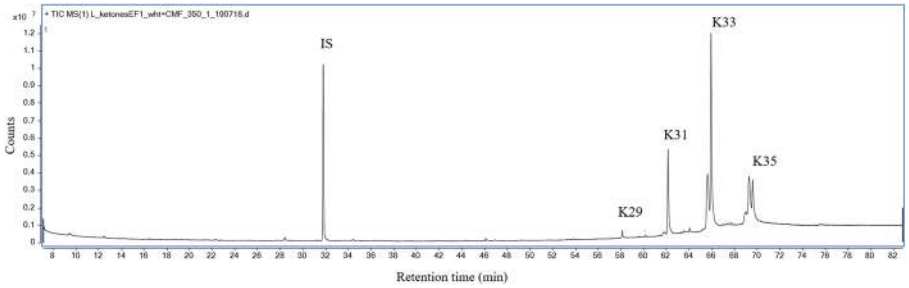

Fig. 15 Formation of abundant saturated long-chain symmetrical and slightly asymmetrical ketones, 14-nonacosanone (K29), 16-hentriacontanone (K31), 16-tritriacontanone (K33), and 18-pentatriacontanone (K35), in previously calcined cow bone treated with fresh cow marrow fat and reheated under oxygen reduced conditions at 350 °C, 60 min. Before reheating with fresh cow fat, the previously calcined bone had no detectable ketones and very low amounts of lipids overall (Tables 1 and 3)

The greatest amounts of pyrolysis products, saturated long-chain symmetrical and asymmetrical ketones, short-chain alkanes, γ-lactones, and nitriles were present in the black layer of the cow bone fire, and in the 350 °C muffle furnace experiments. Only very small amounts of lipids were detected at 400 °C in our muffle furnace experiments and in the white layers of our experimental fires, probably because conditions were not sufficiently anoxic. Previous research has demonstrated that products such as alkanes, ketones, and nitriles form efficiently at temperatures above 400 °C, under anoxic conditions (Ayllón *et al*. 2006; Raven *et al*. 1997; Renz 2005). The formation of long-chain symmetrical and asymmetrical ketones is also known to be catalyzed by metal oxides (Pham *et al*. 2013; Raven *et al*. 1997; Renz 2005), which were present in the mafic basalt substrate and the calcined bones. However, the white layer of the fires experienced the highest temperatures and the most oxic conditions, leading to nearly complete combustion of organics. The black layer, which formed beneath the white layer and in association with the first few millimeters of the mineral sediment, presumably experienced lower oxygen conditions that were more conducive to pyrolysis. Additionally, the natural tendency of the heated and liquified fats would be to travel downward, so the greatest amounts of precursor molecules would be concentrated below the calcined bones.

As evidenced by the macroscopic profile, micromorphological analysis, and molecular analysis, a large amount of heated and liquified fat also penetrated several centimeters into the basalt sediment to form the brown layer. In molecular content, the brown layer appeared to be less affected by heat than the black layer. The brown layer did contain a range of pyrolyzed molecules, but these were fewer in number and in lower concentrations than in the black layer (Tables 1 and 3). In addition to fewer pyrolytic biomarkers, fewer oxidation products such as dicarboxylic acids, were also present. Further, the fatty acid distribution in the brown layer more closely resembled fresh cow fat as it retained higher proportions of $C_{18:1}$, a monounsaturated fatty acid, than the saturated fatty acid, $C_{18:0}$ (Fig. 11).

The experimental pine wood fire left behind few diagnostic lipids other than small amounts of methyl dehydroabietate and stigmasten-3,5-diene. The main defining characteristic of our experimental pine wood fire, with respect to the cow bone fire, was the very low amount of lipid added to the sediments. Also, contrary to Lejay *et al*. (2016), we did not find that aromatics like various benzene products were confined to our wood fire. In fact, we did not detect these in the ash layer or the black layer of our wood fire at all, but did detect them in the cow bone fire and in laboratory heating experiments of cow marrow fat. Their absence in the former may be attributed to the high burning efficiency and extremely low amount of lipids introduced to the sediments during our wood fire, as wood smoke is known to contain abundant aromatic components formed from the incomplete combustion of wood (Simoneit 2002). On the other hand, it is important to note that we did detect several aromatic products, alkyl benzenes and alkyl naphthalenes, in our bone fire and in laboratory heating experiments involving only cow marrow fat and basalt sediment (Tables 1, 2, and 3). Aromatic compounds such as these are also known to form in pyrolyzed animal fats and plant oils during cooking and the production of biofuels (probably through Diels-Alder reactions involving unsaturated fatty acids) (Alencar *et al*. 1983; Ben Hassen-Trabelsi *et al*. 2014; Schwab *et al*. 1988). This provides clarification that formation of aromatic compounds is not confined to the burning of wood fuel.

Thermal Effects on $\delta^{13}C$ Values of Fatty Acids for Cow Bone Fire, Cow Marrow Fat Heating Sequence, and Pine Wood Fire

Figure 16 shows the $\delta^{13}C$ values of $C_{16:0}$ and $C_{18:0}$ from fresh cow bone marrow fat at room temperature, and cow marrow fat from the same sample after heating it to 300 °C and 350 °C. Not enough material remained at 400 °C to accurately measure $\delta^{13}C$ values. Little difference is apparent between unheated cow marrow fat and the same cow fat heated at 300 °C. At 350 °C, however, there is a shift to slightly more enriched $\delta^{13}C$ values (less than 1 ppm, Table 4). Likewise, a small enrichment has previously been noted in $\delta^{13}C$ values of many alkanes heated over a similar temperature range, with a jump to 3–4 ppm at temperatures above 450 °C (Jambrina-Enríquez *et al*. 2018). Different starting $\delta^{13}C$ values for unheated cow bone fat in the heating sequence (Fig. 16) and the experimental cow bone fire (Fig. 17) can probably be attributed to different animal sources. The laboratory sequence used fat from a single cow femur purchased from a local grocery store in Tenerife; the experimental fire used bones from a different cow obtained from a local butcher. It seems likely that these animals had different dietary compositions in life, with one possibly consuming more maize or other C4 plant material. Despite different starting values, source material was kept constant for each experimental series and the resulting enrichment patterns are consistent with one another.

Heating should favor vaporization of the lighter isotopic compound over the heavier isotopic compound, and may be responsible for the slight enrichment observed in the fatty acids heated above 300 °C. This is a general trend in the isotopic fractionation between the condensed or gaseous form of light stable isotopes (Poole *et al*. 2002). Isotopically heavier versions of organic compounds have lower vapor pressure than the isotopically lighter versions of the same compounds and are preferentially retained in the condensed phase (Cappa *et al*. 2003; Hoefs 2013:9).

Kinetic effects may also act to enrich ^{13}C in the unreacted fatty acids. These effects involve differences in the rate of a chemical reaction for a heavy or lighter version of the same element. In unidirectional reactions, such as pyrolysis or combustion, the light isotope should be favored in reaction products (Hoefs 2013:10–12). This would tend to increase the concentration of ^{13}C in the pool of unreacted fatty acids. At the same time, this predicts that products of pyrolysis such as heptadecane and long-chain symmetrical and slightly asymmetrical ketones should be depleted in $\delta^{13}C$ relative to their precursor fatty acids.

Figure 17 shows unburned CMF, followed by the $\delta^{13}C$ values of $C_{16:0}$ and $C_{18:0}$ for residues from the brown, black, and white layers of the bone fire. It also plots the values for unburned wood, followed by residues from the black layer and the white (ash and charcoal) layer. Here, we can see that the shorter fatty acid ($C_{16:0}$) appears to be more enriched in ^{13}C than the longer fatty acid ($C_{18:0}$). Also, the white layer is more enriched in ^{13}C than the black layer (presumably because this layer represents the remains of a hotter portion of the hearth). The fatty acids are enriched up to 2 ppm in the white layers, and 1 ppm or less in the black layers (Table 5). Standard deviations for replicate measurements were generally less than 0.2 ppm and can be found in supplemental materials.

Implications for Recognizing Bone Fires in Archaeological Contexts

The results presented here indicate that combining sedimentary, molecular, and isotopic data can improve the recognition of bone fires in archaeological contexts. Bone fires added a large amount of lipids to the sediment and this traveled several centimeters below the surface as shown by the presence of tarry black coatings and microscopic massive black infillings up to 1 cm (corresponding to the black layer), darkening observed down to 4 cm in the macroscopic profile (corresponding to the brown layer), and specific molecular and isotopic evidence in both the black and brown layers. This type of input did not occur with the pine wood fire. Contributions were several orders of magnitude lower and sub-surface organic coatings were not present on mineral surfaces in the pine wood fire. Unlike the pine wood fire, no reddening of the mineral sediment beneath the bone fire was observed. This may reflect the lower maximum temperatures reached by the sediments beneath the bone fire. The lower temperatures recorded in sediments beneath the bone fire and lack of reddening lends support to observations made in several previous studies (Crass *et al*. 2011; Théry-Parisot 2002) that characterized bone as a poor conductor of heat (but see Lejay *et al*. 2016). It is also worth noting that the extracellular matrix of wood is composed of materials that burn and release heat (cellulose, hemicellulose, and lignin) (Anderson 1958); in contrast to this, the extracellular matrix of bone is largely composed of mineral material (hydroxyapatite) that does not burn. Temperate wood, on average, contains 1% ash or mineral content (Pettersen 1984) while mammalian bone, on average, contains 60–70% mineral content by weight (Boskey 2013). This means that nearly the entirety of wood burns, the volatile organic components as well as the matrix. In bone, the mineral scaffolding serves as a container but does not generate heat, it is primarily the fat which burns (along with some protein). As others have noted, bone fires are essentially grease fires and most of the heat is transmitted upward and out as radiant heat and through convection (Crass *et al*. 2011; Théry-Parisot 2002). Another factor which may reduce oxidation of the sediments beneath a bone fire is the large amount of fat which leaks into the sediments. If sediments are coated with lipids, this would limit mineral surface contact with both water and oxygen—key players in oxidation.

One additional observation deserves further discussion. Microscopically, there was an absence in the bone fire thin section of vesicular glassy black material—material that is commonly described as "fat-derived char" (Berna and Goldberg 2007; Goldberg *et al*. 2009; Mallol *et al*. 2013; Mallol and Henry 2017). Although massive black coatings resembling asphalt were present in the uppermost millimeters of the deposit (Figs. 5c and 7), no char was noted in microscopic thin section (Fig. 7). Based on these visual observations, as well as the molecular content, this material can be better described as fat-derived tar, or bio-oil (Ayllón *et al*. 2006; Ben Hassen-Trabelsi *et al*. 2014).

Ben Hassen-Trabelsi *et al*. 2014 note that bio-char has a more oxygenated and less aliphatic character than bio-oil (p. 217), and Ayllón *et al*. 2006 note that bio-char increases in surface area and becomes more brittle and resistant to melting at higher temperatures (above 600 °C). It could be that hotter conditions will increase the presence and visibility of char. We wonder if such fat-derived char might be formed differently in fires containing greater amounts of wood. If this is true, then the presence of char as well as molecular markers of animal fat could be an indication of hotter fires

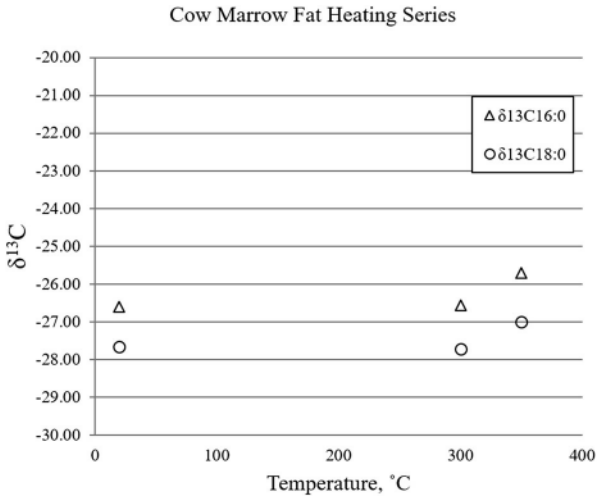

Fig. 16 $\delta^{13}C$ values of saturated fatty acids $C_{16:0}$ and $C_{18:0}$ from cow fat heating series

that contain a higher proportion of wood, while the presence of amorphous black material, no char, and molecular markers of animal fat would be associated with fires containing very high proportions of bone or animal fat as fuel.

Biomarkers of Animal Fat Pyrolysis

As described in the results section, a series of saturated long-chain symmetrical and slightly asymmetrical ketones form by heating saturated fatty acids and triglycerides at high temperatures. These are known to form most readily in the presence of divalent metal cations and conditions of reduced oxygen (Pham *et al.* 2013; Raven *et al.* 1997; Renz 2005). The formation of these molecules from animal fats has been the subject of several studies in experimental and archaeological pottery (Baeten *et al.* 2013; Evershed *et al.* 1995; Raven *et al.* 1997), but conditions of their formation, and their potential to serve as biomarkers in hearth sediments are still poorly understood (though see Lejay *et al.* 2016; March *et al.* 2014). Our experiments show that these molecules form in basalt sediments (Fig. 13, Tables 2 and 3). They also form exceptionally well in

Table 4 Changes in δ13C values of cow marrow fat with heating

Temp (°C)	$\delta^{13}C_{16:0}$	$\delta^{13}C_{18:0}$	$\Delta_{16:0}$[a]	$\Delta_{18:0}$[a]
20	−26.60	−27.67		
300	−26.57	−27.73	0.03	−0.06
350	−25.69	−27.00	0.91	0.67

Note: Laboratory heating experiments (Table 4) versus the outdoor bone fire (Table 5) used bones from two different animals. Differences in the starting $\delta^{13}C$ values of unheated cow marrow fat in the two series are probably due to dietary differences. In this case, the cow bones used for the outdoor bone fire appear to be from an animal that consumed a diet higher in maize or another C4 plant

[a] Δ 16:0 and Δ 18:0 show the change in δ13C values of C16:0 and C18:0 in the heated samples relative to the corresponding fresh starting material

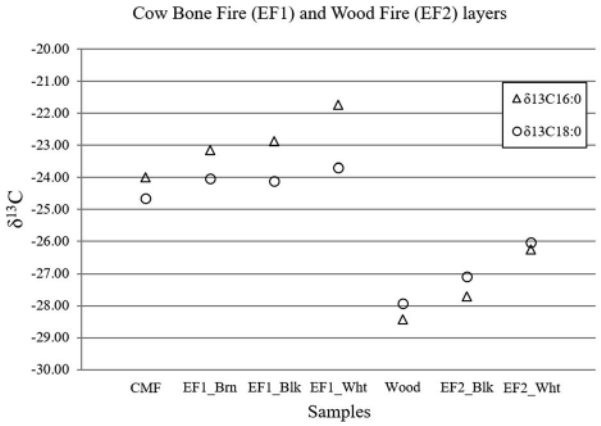

Fig. 17 $\delta^{13}C$ values of saturated fatty acids $C_{16:0}$ and $C_{18:0}$ for fresh starting material and layers of the experimental fires

previously calcined bone to which additional fat has been added and reheated (Fig. 15). These long-chain symmetrical and slightly asymmetrical ketones are good candidates for biomarkers of burned animal fat in hearth sediments for three reasons: (1) they have a high potential for preservation; (2) several individual compounds, and especially the combinations and relative proportions in which they form, are unusual in nature; (3) because we know how they form, they can provide source information and can be tied to human activities. Each of these points is discussed below.

First, based on their structure and on experimental data, saturated long-chain symmetrical and slightly asymmetrical ketones are predicted to have higher preservation potential than most other lipids, except long-chain alkanes (Cranwell 1981; Moucawi *et al*. 1981). They are highly hydrophobic and unlikely to move in a sediment column. Additionally, the placement of the carbonyl group between two long aliphatic chains may sterically hinder availability of the carbonyl group to participate in chemical reactions. Moucawi *et al*. (1981) found that octacosane (a 28-

Table 5 δ13C values for sediments from bone and wood fires

Sample	$\delta^{13}C_{16:0}$	$\delta^{13}C_{18:0}$	$\Delta\ C_{16:0}$[a]	$\Delta\ C_{18:0}$[a]
CMF[b]	−23.99	−24.65		
EF1_Brn	−23.15	−24.04	0.84	0.61
EF1_Blk	−22.87	−24.12	1.12	0.53
EF1_Wht	−21.74	−23.69	2.25	0.96
Wood[c]	−28.42	−27.93		
EF2_Blk	−27.71	−27.09	0.71	0.84
EF2_Wht	−26.25	−26.04	2.17	1.89

[a] Δ 16:0 and Δ 18:0 show the change in δ13C values of C16:0 and C18:0 in the fire layers versus the corresponding fresh starting material

[b] CMF is the averaged value of fresh, unburned cow fat from two samples of bone used in the bone fire

[c] Wood is the averaged value for two unburned pieces of the wood used in the pine wood fire

carbon *n*-alkane) and 14-heptacosanone (a 27-carbon symmetric ketone) decompose to a similar extent in experimental soils, while 3-octadecanone, a shorter chain ketone with the carbonyl group in the 3-position, toward the end of the molecule, was degraded to a much higher degree.

Second, combinations and relative proportions of saturated long-chain symmetrical and slightly asymmetrical ketones formed from heating animal fat are not typical of plant waxes (references in Raven *et al*. 1997:268–269). Leaf waxes tend to be dominated by a single symmetrical long-chain ketone rather than co-dominant mixtures of several long-chain symmetrical and slightly asymmetrical ketones. Also, the slightly asymmetrical ketones 14-nonacosanone and 16-tritriacontanone are unusual in plants. Due to biosynthetic pathways, long-chain ketones in leaf waxes are usually symmetric (Kolattukudy *et al*. 1976) and tend to contain the same dominant carbon number alkane as the dominant long-chain symmetrical ketone (Walton 1990). An absence of long-chain alkanes of similar number would be further evidence for formation from heated animal fat. This is especially true since similar chain length alkanes are predicted to have greater preservation potential than long-chain symmetrical ketones (Cranwell 1981, Moucawi *et al*. 1981).

Third, long-chain symmetrical and slightly asymmetrical ketones preserve information about the predominant fatty acids present in the original source material (animal fat), and they tell us that it was exposed to high temperatures (generally above 300 °C). Because they form through a simple reaction between two precursor fatty acids (rather than a complex chain of reactions involving external input), the structure of long-chain ketones can tell us about the structures of the precursor molecules (Baeten *et al*. 2013; Pham *et al*. 2013; Raven *et al*. 1997; Renz 2005). It should also be possible to reconstruct the $\delta^{13}C$ values of the original fatty acids based on the $\delta^{13}C$ values of the long-chain ketones—though more research is required to test expected patterns. The ability to combine patterns of long-chain ketone formation with corresponding $\delta^{13}C$ values could provide strong evidence for the presence of burned animal fat in ancient combustion features and may be able to separate major groups of animal sources, much like CSIA of fatty acids can in more recent hearth sediments and pottery sherds (Anderson *et al*. 2017; Buonasera *et al*. 2015; Evershed *et al*. 2002b).

Comparisons of our experimental hearth sediments (produced from burned/heated cow marrow fat) with sediments from an archaeological combustion feature dominated by marine mammal bone provide further clarification of the possibilities of using long-chain symmetrical and slightly asymmetrical ketones to identify sources of animal fats. In this case, archaeological residues were extracted from a burned bone feature associated with a late Birnirk house at Cape Espenberg (*ca.* AD 1150) in northwestern Alaska (Alix and Mason 2018). The source of the archaeological lipids was identified as marine animal based on separate molecular and isotopic evidence including presence of several isoprenoid fatty acids, ω-(*o*-alkylphenyl) alkanoic acids 20 and 22 carbons long and $\delta^{13}C$ values of fatty acids. This feature was also associated with a large proportion of sea mammal bones (Alix and Mason 2018). (In-depth discussion of the Alaskan molecular and isotopic data in their archaeological and experimental context will be presented in a forthcoming publication.)

Consistent with the prior molecular, isotopic, and osteofaunal data, we found that the long-chain ketones preserved in the archaeological materials were reflective of heated marine mammal fat (Fig. 18). Marine mammal fat contains a high amount of the

saturated fat $C_{16:0}$ and also $C_{14:0}$, and much lower relative amounts of $C_{18:0}$. Ketonic decarboxylation between two $C_{14:0}$ fatty acids produces 14-heptacosanone, while 14-nonacosanone is formed from ketonic decarboxylation between $C_{16:0}$ and $C_{14:0}$ fatty acids, and 16-hentiracontanone forms from this same reaction between two $C_{16:0}$ fatty acids. Correspondingly, the dominant ketone in the archaeological sample was 14-heptacosanone (K27), 14-nonacosanone (K29), and 16-hentriacontanone (K31) (Fig. 18). In contrast, our samples of burned and heated cow fat contained mainly 16-hentriacontanone (K31), 16-tritriacontanone (K33), and 18-pentatriacontanone (K35), plus a small amount of 14-nonacosanone (Figs. 13 and 15).

Because mineral surfaces that contain divalent metal oxides are believed to function as catalysts in the formation of long-chain symmetrical ketones from fatty acid precursors (see the section, *Molecular Data for the Bone Fire (EF1) and Cow Marrow Fat Heating Sequence*), different mineral substrates could be expected to affect the rate of ketone formation, but not the specific end products. Following this line of reasoning, calcitic sediments, or iron-containing sediments might produce greater amounts of long-chain symmetrical and slightly asymmetrical ketones than sediments composed of quartz sand. This is an area that deserves further experimentation and archaeological testing.

It is also important to note that, in our fire experiments, long-chain ketones formed from burning animal fats but not from burning wood. This is probably related to several factors. First, all indications are that our experimental wood fire burned under highly oxic conditions—conditions that would be conducive to efficient combustion rather than pyrolysis. Second, detectable amounts long-chain symmetrical ketones are less likely to form from wood than from animal fat because saturated fatty acids are present in very low concentrations in wood tissues (Anderson 1958; Zinkel 1989) while animal fats are composed almost entirely of fatty acids (as triglycerides) with large amounts of the saturated fatty acids $C_{18:0}$, $C_{16:0}$, and C_{14}. Further, because the primary saturated fatty acid in wood is $C_{16:0}$ with very low amounts of $C_{18:0}$ or $C_{14:0}$ (Saranpää and Nyberg 1987; Zinkel 1989), any saturated long-chain ketones that did form should consist almost exclusively of 16-hentriacontane (K31). Finally, it is possible that $\delta^{13}C$ values of 16-henitriacontane produced from wood lipids would differ significantly from $\delta^{13}C$ values for the same molecule derived from animal fats. In our experiments, fatty acids from heated marrow fat and the bone fire were noticeably more enriched than those from our wood fire (Figs. 16 and 17, Tables 4 and 5), but additional research on modern and ancient materials from specific contexts is needed.

The predominance of heptadecane, a 17-carbon *n*-alkane among the alkane fraction, may provide additional evidence for the intense heating of animal fats. Heptadecane is the predominant alkane formed from the pyrolysis of terrestrial animal fats, has a high preservation potential, and is not common in terrestrial plant sources (Eckmeier and Wiesenberg 2009). Fresh, unheated terrestrial plant waxes contain long-chain *n*-alkanes, generally maximizing at C_{27}, C_{29}, or C_{31} (Eglinton and Hamilton 1967). Short-chain *n*-alkanes with a maximum at C_{16} and C_{18} are known to form after burning terrestrial plant material, and probably form from degraded leaf waxes (Eckmeier and Wiesenberg 2009; Wiedemeier *et al.* 2015; Wiesenberg *et al.* 2009). In our experiments, heptadecane was the dominant alkane formed from heated cow marrow fat, with very little C_{16} or C_{18} alkanes formed (Fig. 12). This same pattern has been reported in the conversion of animal fats to biofuels (Ben Hassen-Trabelsi *et al.* 2014).

Heptadecane has been shown to form from stearic acid ($C_{18:0}$) that has lost a carboxyl group due to intense heating (Maher and Bressler 2007). As noted previously, plant materials contain little stearic acid, while it is a dominant fatty acid in terrestrial animal fats—especially among ruminants (Evershed *et al*. 2002a).

Heptadecane is, however, a prominent alkane formed by cyanobacteria and algae and is associated with aquatic environments (Dinel *et al*. 1990; Eckmeier and Wiesenberg 2009; Schirmer *et al*. 2010). Alone, heptadecane would not be a robust indicator of burned animal fat, but in combination with other molecules, such as long-chain ketones and $\delta^{13}C$ values of individual molecules (short-chain alkanes and long-chain ketones), it could provide added support for the presence of burned animal fat. Moreover, due to differences in discrimination, animal fats tend to be more enriched than plant fuels from the same environment. In an archaeological context, heptadecane derived from burned animal fat should be more enriched in $\delta^{13}C$ than biomarkers of plant material, such as long-chain alkanes, extracted from the same sediment sample or associated with other sediments from the same layer.

Sampling Combustion Features for Biomarkers and CSIA

To achieve the greatest amount of information, molecular analysis of hearths should be conducted stratigraphically. Combustion features should be carefully excavated and separate bulk samples collected from distinct internal strata. Mallol and Henry (2017) provide guidelines for the excavation and sampling of combustion structures.

We further suggest that the black layer should be a primary target for molecular and isotopic analyses. This layer contains the highest concentration of lipids and greatest number of pyrolysis products. Additionally, carbon isotopic enrichment of fatty acids in the black layer was less than the enrichment detected in the white layer (1 ppm or less). However, separate samples from other layers should also be collected, and samples of unaffected matrix must also be sampled for comparison. Control samples taken stratigraphically from sediments adjacent to a combustion feature can allow for comparison of molecular content and stable isotope values.

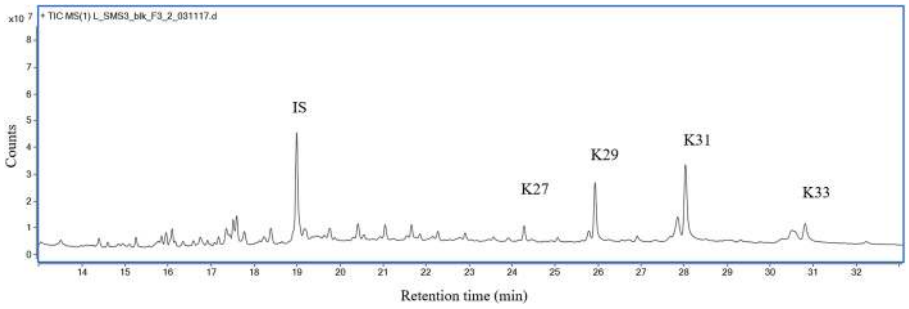

Fig. 18 Saturated long-chain symmetrical and slightly asymmetrical ketones 14-heptacosanone (K27), 14-nonacosanone (K29), 16-hentriacontanone (K31), and 16-tritriacontanone (K33), present in an extract of the upper black layer of stratified burned marine animal bone feature in association with a late Birnirk house (*ca.* AD 1150) in Cape Espenberg, Alaska. The pattern of saturated long-chain symmetrical and slightly asymmetrical ketones is shifted two carbons shorter than the pattern observed in cow fat, reflecting the higher amounts of $C_{14:0}$ and $C_{16:0}$, and lower amounts of $C_{18:0}$ typically present in marine animal fats versus terrestrial animal fats

Comparing the molecular markers and overall lipid content in blackened layers to those in adjacent, overlying, and underlying sediments could provide a better idea about the primary or secondary context of burned animal bones. Materials just below a burned layer, that are in primary context, would be expected to have a higher lipid content than control sediments. Additionally, calcined bone with abundant ketones could indicate that additional materials were burned above the calcined bone layer later in time. If the feature represents multiple fires, the white layer from earlier fires has increased potential to contain abundant ketones and other pyrolysis products from subsequent fires.

Conclusions

Combined molecular, isotopic, and microstratigraphic analyses of combustion features could supply a largely untapped reservoir of information on a variety of issues including occupational history, past climate, fuel management, and cooking practices. Here, we have presented results from experimental bone and wood fires and laboratory heating experiments to better integrate and clarify molecular and isotopic criteria for identifying burned animal fats in combustion-related features. Many of the molecular products formed in bone fires should occur in other combustion-related features where large amounts of animal fats are burned (*e.g.*, various cooking features, cremation features). Yet, differences in the structure, materials involved, and overall formation processes of cooking features or cremations can be expected to yield very different temperature and depositional patterns as well as different proportions or types of biomarker compounds. Additional microcontextualized experiments should be conducted to better interpret a wider range of specific combustion-related activities.

Our predominantly bone-fueled fire did not get as hot as the wood-only fire, and differences were noted in the macroscopic and microscopic sedimentary structure of the two types of fires. The bone fire was capped with a layer of highly fragmented calcined and strongly burnt bone. Beneath this was a thin patchy layer of burned fat that resembled asphalt and which penetrated approximately 1 cm into the inorganic crushed basalt sediment. In comparison, a thin layer of ash and charcoal overlying fine black particulate material was noted for the wood fire. Beneath this, sediments for the wood fire were visibly reddened. Sediments beneath the black layer of the bone fires were not visibly reddened but were characterized by the addition of a tremendous amount of animal fat which penetrated at least 4 cm beneath the surface. This layer of fat may have had a role in protecting the mineral sediments from oxidation.

For the best interpretation, samples for molecular and isotopic analyses should be collected from all distinct stratigraphic layers in a combustion feature, and control samples should be included from adjacent sediments. This practice can link microscopic and molecular data relevant to determining the primary or secondary context of combustion-related sediments and to the presence of multiple burning events. Our data show that the largest quantities and greatest numbers of pyrolyzed molecules are located in the black layers. Stable isotope values for the black layers are also less affected than those in the white layers. This was true for both types of fires, even

though sediments beneath the bone fire contained far greater amounts of lipids and pyrolyzed biomarkers than our wood fire.

We have described here a number of specific lipid biomarker compounds and their likely mechanisms of formation. The combined presence of symmetric and slightly asymmetric saturated long-chain ketones (14-nonacosanone, 16-hentriaconanone, 16-tritriacontanone, and 18-pentatriacontanone), especially together with heptadecane (C_{17} *n*-alkane), are molecular indicators of the thermal degradation of terrestrial animal fat. To better detect these, molecular analysis must target separate fractions, specifically the ketone (F3) and alkane (F1) fractions (as detailed in the methods section), as well as the TLE.

Heptadecane is a major product of the pyrolysis of terrestrial animal fats, and is rare in terrestrial alkanes. However, it is a dominant short-chain alkane in some aquatic sediments and may serve best as a supplementary biomarker for burned animal fat. The most promising biomarkers we encountered for identifying contributions of burned animal fat to combustion-related features are different combinations of specific saturated long-chain symmetrical and slightly asymmetrical ketones formed through pyrolysis of fatty acids. Similar to what has been described in archaeological pottery, these saturated long-chain symmetric and slightly asymmetric ketones were formed in combustion-related sediments (basalt and previously calcined bone) by heating animal fats to temperatures above 300 °C. Association of these molecules in black layers of features determined to be remains of ancient fireplaces (or suspected of being combustion related) can provide evidence for cooking or burning of fatty animal materials. The combinations formed from burned animal fat are not typical of plant waxes and are unlikely to be introduced from post-depositional sources. The ability to trace formation of these molecules to a human activity, namely burning, is especially important in Middle Paleolithic contexts or other settings where it may not be possible to get a reliable radiocarbon date directly on the organic residues. Further, we show that the dominance of specific long-chain symmetric and slightly asymmetric ketones reflects the original distribution of dominant saturated fatty acids present in source materials (terrestrial animal fats or marine animal fats) extracted from experimental sediments and archaeological sediments. The ability to combine patterns of long-chain ketone formation with CSIA would provide strong evidence for the presence of burned animal fat in ancient combustion features and may provide a means of separating major groups of animal sources, much like CSIA of fatty acids can presently.

Acknowledgments This research was supported by European Research Council Consolidator Grant, *Insights into the Neanderthals and their demise from the study of microscopic and molecular charred matter in Middle Paleolithic sediments* (ERC-CoG-2014-PALEOCHAR). We are thankful to the many people at AMBI Lab (Archaeological Micromorphology and Biomarker Lab) who contributed to this research. In particular, micromorphological blocks were prepared from difficult substrates by Caterina Rodriguez De Vera, and a preliminary test of bone burning was accomplished with the efforts of Rory Connolly and Lucia Leierer. We are grateful to José Antonio Palenzuela López for synthesizing several ketone standards that were difficult to obtain from vendors. We also appreciate conversations with Margarita Jambrina Enriquez about alkanes and stable isotope values. Finally, we thank Jelmer Eerkens and three anonymous reviewers for their comments and suggestions which have improved the clarity of the manuscript.

References

Aldeias, V., Dibble, H. L., Sandgathe, D., Goldberg, P., & McPherron, S. J. P. (2016). How heat alters underlying deposits and implications for archaeological fire features: A controlled experiment. *Journal of Archaeological Science, 67*, 64–79.

Alencar, J. W., Alves, P. B., & Craveiro, A. A. (1983). Pyrolysis of tropical vegetable oils. *Journal of Agricultural and Food Chemistry, 31*(6), 1268–1270.

Alix, C., & Mason, O. (2018). Birnirk prehistory and the emergence of Inupiaq culture in northwestern Alaska: Archaeological and anthropological perspectives. Field Investigations at Cape Espenberg, 2017. Annual Report to the National Park Service U.S. Department of the Interior.

Anderson, A. B. (1958). The composition and structure of wood. *Journal of Chemical Education, 35*(10), 487.

Anderson, S. L., Tushingham, S., & Buonasera, T. Y. (2017). Aquatic adaptations and the adoption of arctic pottery technology: Results of residue analysis. *American Antiquity, 82*(3), 452–479.

Ayllón, M., Aznar, M., Sánchez, J. L., Gea, G., & Arauzo, J. (2006). Influence of temperature and heating rate on the fixed bed pyrolysis of meat and bone meal. *Chemical Engineering Journal, 121*(2), 85–96.

Baeten, J., Jervis, B., De Vos, D., & Waelkens, M. (2013). Molecular evidence for the mixing of meat, fish and vegetables in Anglo-Saxon coarseware from Hamwic, UK. *Archaeometry, 55*(6), 1150–1174.

Ben Hassen-Trabelsi, A., Kraiem, T., Naoui, S., & Belayouni, H. (2014). Pyrolysis of waste animal fats in a fixed-bed reactor: Production and characterization of bio-oil and bio-char. *Waste Management, 34*(1), 210–218.

Berna, F., & Goldberg, P. (2007). Assessing Paleolithic pyrotechnology and associated hominin behavior in Israel. *Israel Journal of Earth Sciences, 56*(2), 107–121.

Boskey, A. L. (2013). Bone composition: Relationship to bone fragility and antiosteoporotic drug effects. *BoneKEy Reports, 2*(447), 1–11.

Buonasera, T. Y., Tremayne, A. H., Darwent, C. M., Eerkens, J. W., & Mason, O. K. (2015). Lipid biomarkers and compound specific δ13C analysis indicate early development of a dual-economic system for the Arctic Small Tool tradition in northern Alaska. *Journal of Archaeological Science, 61*, 129–138.

Burch, E. S. (1972). The caribou/wild reindeer as a human resource. *American Antiquity, 37*(3), 339–368.

Busse, M. D., Shestak, C. J., Hubbert, K. R., Knapp, E. E. (2010). Soil physical properties regulate lethal heating during burning of woody residues. *Soil Science Society of America Journal, 74*(3), 947–955. https://doi.org/10.2136/sssaj2009.0322.

Cappa, C. D., Hendricks, M. B., DePaolo, D. J., & Cohen, R. C. (2003). Isotopic fractionation of water during evaporation. *Journal of Geophysical Research, 108*(D16), 4525.

Chaiwong, K., Kiatsiriroat, T., Vorayos, N., & Thararax, C. (2013). Study of bio-oil and bio-char production from algae by slow pyrolysis. *Biomass and Bioenergy, 56*, 600–606.

Chang, C. C., & Wan, S. W. (1947). China's motor fuels from tung oil. *Industrial and Engineering Chemistry, 39*(12), 1543–1548.

Choy, K., Potter, B. A., McKinney, H. J., Reuther, J. D., Wang, S. W., & Wooller, M. J. (2016). Chemical profiling of ancient hearths reveals recurrent salmon use in Ice Age Beringia. *Proceedings of the National Academy of Sciences of the United States of America, 113*(35), 9757–9762.

Church, R. R., & Lyman, R. L. (2003). Small fragments make small differences in efficiency when rendering grease from fractured artiodactyl bones by boiling. *Journal of Archaeological Science, 30*(8), 1077–1084.

Copley, M. S., Hansel, F. A., Sadr, K., & Evershed, R. P. (2004). Organic residue evidence for the processing of marine animal products in pottery vessels from the pre-colonial archaeological site of Kasteelberg D east, South Africa. *South African Journal of Science, 100*(5–6), 279–283.

Costamagno, S. (2013). Bone grease rendering in Mousterian contexts: The case of Noisetier Cave (Fréchet-Aure, Hautes-Pyrénées, France). In J. L. Clark & J. D. Speth (Eds.), *Zooarchaeology and modern human origins* (pp. 209–225). Dordrecht: Springer.

Costamagno, S., & Théry-Parisot, I. (2002). Taphonomic consequences of the use of bones as fuel: Experimental data and archaeological applications. In P. Rowley-Conwy, U. Albarella, & K. Dobney (Eds.), *Proceedings of the 9th Conference of the International Council of Archaeozoology, Durham* (pp. 51-62).

Courty, M.-A., Goldberg, P., & Macphail, R. (1990). *Soils and micromorphology in archaeology*. Cambridge: Cambridge University Press.

Cranwell, P. A. (1981). Diagenesis of free and bound lipids in terrestrial detritus deposited in a lacustrine sediment. *Organic Geochemistry, 3*(3), 79–89.

Crass, B. A., Kedrowski, B. L., Baus, J., & Behm, J. A. (2011). Residue analysis of bone-fueled Pleistocene hearths. In T. Gobel & I. Buvit (Eds.), *From the Yenesei to the Yukon: Interpreting lithic assemblage variability in Late Pleistocene/Early Holocene Beringia* (pp. 192–198). College Station: Texas A & M University Press.

Darwent, C. M. (2001). *High Arctic Paleoeskimo fauna: Temporal changes and regional differences (Canada, Greenland)* (Ph.D. dissertation). Department of Anthropology, University of Missouri-Columbia.

DeNiro, M. J., & Epstein, S. (1977). Mechanism of carbon isotope fractionation associated with lipid synthesis. *Science, 197*(4300), 261–263.

Dinel, H., Schnitzer, M., & Mehuys, G. R. (1990). Soil lipids: Origin, nature, content, decomposition, and effect on soil physical properties. In J. Bollag & G. Stotzky (Eds.), *Soil biochemistry* (Vol. 6, pp. 397–429). New York: Marcel Dekker, Inc..

Eckmeier, E., & Wiesenberg, G. L. B. (2009). Short-chain n-alkanes (C16–20) in ancient soil are useful molecular markers for prehistoric biomass burning. *Journal of Archaeological Science, 36*(7), 1590–1596.

Eglinton, G., & Hamilton, R. J. (1967). Leaf epicuticular waxes. *Science, 156*(3780), 1322–1335.

Evershed, R. P., Stott, A. W., Raven, A., Dudd, S. N., Charters, S., & Leyden, A. (1995). Formation of long-chain ketones in ancient pottery vessels by pyrolysis of acyl lipids. *Tetrahedron Letters, 36*(48), 8875–8878.

Evershed, R. P., Dudd, S. N., Copley, M. S., Berstan, R., Stott, A. W., & Mottram, H. (2002a). Chemistry of archaeological animal fats. *Accounts of Chemical Research, 35*(8), 660–668.

Evershed, R. P., Dudd, S. N., Copley, M. S., & Mutherjee, A. (2002b). Identification of animal fats via compound specific δ13C values of individual fatty acids: Assessments of results for reference fats and lipid extracts of archaeological pottery vessels. *Documenta Praehistorica, 29*, 73–96.

Evershed, R. P., Copley, M. S., Dickson, L., & Hansel, F. A. (2008). Experimental evidence for the processing of marine animal products and other commodities containing polyunsaturated fatty acids in pottery vessels. *Archaeometry, 50*(1), 101–113.

Forney, F. W., & Markovetz, A. J. (1971). The biology of methyl ketones. *Journal of Lipid Research, 12*(4), 383–395.

Frink, L., & Giordano, C. (2015). Women and subsistence food technology: The Arctic seal poke storage system. *Food and Foodways, 23*(4), 251–272.

García-Piquer, A., Lozano, J.-M., March, R. J., & Estévez-Escalera, J. (2018). An experimental ethnoarchaeology and analytical approach to fire-related management strategies in a hunter-fisher-gatherer society from the southern tip of Tierra del Fuego (Argentina). Ethnoarchaeology (pp. 1–20).

Goldberg, P., Miller, C. E., Schiegl, S., Ligouis, B., Berna, F., Conard, N. J., & Wadley, L. (2009). Bedding, hearths, and site maintenance in the Middle Stone age of Sibudu cave, KwaZulu-Natal, South Africa. *Archaeological and Anthropological Sciences, 1*(2), 95–122.

Halffman, C. M., Potter, B. A., McKinney, H. J., Finney, B. P., Rodrigues, A. T., Yang, D. Y., & Kemp, B. M. (2015). Early human use of anadromous salmon in North America at 11,500 y ago. *Proceedings of the National Academy of Sciences of the United States of America, 112*(40), 12344–12348.

Hansel, F. A., & Evershed, R. P. (2009). Formation of dihydroxy acids from Z-monounsaturated alkenoic acids and their use as biomarkers for the processing of marine commodities in archaeological pottery vessels. *Tetrahedron Letters, 50*(40), 5562–5564.

Hansel, F. A., Copley, M. S., Madureira, L. A. S., & Evershed, R. P. (2004). Thermally produced ω-(o-alkylphenyl) alkanoic acids provide evidence for the processing of marine products in archaeological pottery vessels. *Tetrahedron Letters, 45*(14), 2999–3002.

Heron, C., & Evershed, R. P. (1993). The analysis of organic residues and the study of pottery use. *Archaeological Method and Theory, 5*, 247–284.

Heron, C., Nilsen, G., Stern, B., Craig, O., & Nordby, C. (2010). Application of lipid biomarker analysis to evaluate the function of "slab-lined pits" in Arctic Norway. *Journal of Archaeological Science, 37*(9), 2188–2197.

Herrera-Herrera, A. V., & Mallol, C. (2018). Quantification of lipid biomarkers in sedimentary contexts: Comparing different calibration methods. *Organic Geochemistry, 125*, 152–160.

Hoefs, J. (2013). *Stable isotope geochemistry* (7th ed.). New York: Springer.

Holmes, C. E. (2001). Tanana River Valley archaeology circa 14,000 to 9000 B.P. *Arctic Anthropology, 38*(2), 154–170. https://doi.org/10.1016/j.orggeochem.2018.07.009.

Jambrina-Enríquez, M., Herrera-Herrera, A. V., & Mallol, C. (2018). Wax lipids in fresh and charred anatomical parts of the Celtis australis tree: Insights on paleofire interpretation. *Organic Geochemistry, 122*, 147–160.

Jones, K. T., & Metcalfe, D. (1988). Bare bones archaeology: Bone marrow indices and efficiency. *Journal of Archaeological Science, 15*(4), 415–423.

Karr, L. P., Outram, A. K., & Adrien Hannus, L. (2010). A chronology of bone marrow and bone grease exploitation at the Mitchell Prehistoric Indian Village. *Plains Anthropologist, 55*(215), 215–223.

Kedrowski, B. L., Crass, B. A., Behm, J. A., Luetke, J. C., Nichols, A. L., Moreck, A. M., & Holmes, C. E. (2009). GC/MS analysis of fatty acids from ancient hearth residues at the Swan Point archaeological site. *Archaeometry, 51*(1), 110–122.

Kent, S. (1993). Variability in faunal assemblages: The influence of hunting skill, sharing, dogs, and mode of cooking on faunal remains in a sedentary Kalahari community. *Journal of Anthropological Archaeology, 12*(4), 323–385.

Kim, S. W., Koo, B. S., & Lee, D. H. (2014). A comparative study of bio-oils from pyrolysis of microalgae and oil seed waste in a fluidized bed. *Bioresource Technology, 162*, 96–102.

Kolattukudy, P. E., Croteau, R., & Buckner, J. S. (1976). Biochemistry of plant waxes. In P. E. Kolattukudy (Ed.), *Chemistry and biochemistry of natural waxes* (pp. 289–347). New York: Elsevier.

Leechman, D. (1951). Bone grease. *American Antiquity, 16*(4), 355–356.

Lejay, M., Alexis, M., Quénéa, K., Sellami, F., & Bon, F. (2016). Organic signatures of fireplaces: Experimental references for archaeological interpretations. *Organic Geochemistry, 99*, 67–77.

Logan, J. M., Jardine, T. D., Miller, T. J., Bunn, S. E., Cunjak, R. A., & Lutcavage, M. E. (2008). Lipid corrections in carbon and nitrogen stable isotope analyses: Comparison of chemical extraction and modelling methods. *The Journal of Animal Ecology, 77*(4), 838–846.

Lucquin, A. (2007). *Étude physico-chimique des méthodes de cuisson pré et protohistoriques*. (Ph.D. dissertation). Université Rennes 1, France.

Lucquin, A. (2016). Untangling complex organic mixture in prehistoric hearths. *Proceedings of the National Academy of Sciences of the United States of America, 113*(38), 10456–10457.

Lupo, K., & Schmidt, D. N. (1997). Experiments in bone boiling: Nutritional returns and archaeological reflections. *Anthropozoologica, 95-96*, 138–144.

Ma, F., & Hanna, M. A. (1999). Biodiesel production: A review. *Bioresource Technology, 70*, 1–15.

Maher, K. D., & Bressler, D. C. (2007). Pyrolysis of triglyceride materials for the production of renewable fuels and chemicals. *Bioresource Technology, 98*(12), 2351–2368.

Maher, K. D., Kirkwood, K. M., Gray, M. R., & Bressler, D. C. (2008). Pyrolytic decarboxylation and cracking of stearic acid. *Industrial & Engineering Chemistry Research, 47*(15), 5328–5336.

Mallol, C., & Henry, A. (2017). Ethnoarchaeology of Paleolithic fire: Methodological considerations. *Current Anthropology, 58*, S16. https://doi.org/10.1086/691422.

Mallol, C., Hernández, C. M., Cabanes, D., Machado, J., Sistiaga, A., Pérez, L., & Galván, B. (2013). Human actions performed on simple combustion structures: An experimental approach to the study of Middle Palaeolithic fire. *Quaternary International: The Journal of the International Union for Quaternary Research, 315*, 3–15.

Manne, T. (2010). *Upper Paleolithic foraging decisions and early economic intensification at Vale Boi, Southwestern Portugal*. (Ph.D. dissertation) Department of Anthropology, University of Arizona. https://arizona.openrepository.com/handle/10150/204309. Accessed 7 Apr 2017

Manne, T. (2014). Early Upper Paleolithic bone processing and insights into small-scale storage of fats at Vale Boi, southern Iberia. *Journal of Archaeological Science, 43*, 111–123.

March, R. J. (1999). Chimie organique appliquée à l'étude des structures de combustion du site de Tunel I (Terre de Feu, Argentine). *Revue d'archéométrie, 23*, 127–156.

March, R. J. (2013). Searching for the functions of fire structures in Eynan (Mallaha) and their formation processes: A geochemical approach. In O. Bar-Yosef & F. R. Valla (Eds.), *Natufian foragers in the Levant: Terminal Pleistocene social changes in Western Asia* (Vol. 19, pp. 227–283). Ann Arbor: International Monographs in Prehistory.

March, R. J., & Lucquin, A. (2006). About cooking and firing: Chemical analysis of fat residues from experimental and archaeological data. XIVe Congrès UISPP, Liège 3–8 Septembre 2001 Section 1.

Colloque The Signifiance of Experimentation for the Interpretation of the Archaeological Processes: *Methods, Problems and Projects*, Maria Rosa Iorvino-BAR, 30 p.

March, R. J., Baldessari, A., & Gross, E. G. (1989). Determinacion de compuestos orgánicos en estructuras de combustión arqueológicas. In M. Olive & Y. Taborin (Eds.), *Nature et Fonction des foyers préhistoriques, Actes du colloque international de Nemours (1987)* (pp. 47–58). Nemours: APRAIF.

March, R. J., Lucquin, A., Joly, D., Ferreri, J. C., & Muhieddine, M. (2014). Processes of formation and alteration of archaeological fire structures: Complexity viewed in the light of experimental approaches. *Journal of Archaeological Method and Theory, 21*(1), 1–45.

McCullough, D. R., & Ullrey, D. E. (1983). Proximate mineral and gross energy composition of white-tailed deer. *The Journal of Wildlife Management, 47*(2), 430–441.

McMurry, J. (1992). *Organic chemistry* (3rd ed.). Pacific Grove: Brooks/Cole.

Mentzer, S. M. (2009) Bone as a fuel source: The effects of initial fragment size distribution. In E. Cappellini, A. Prohaska, F. Racimo, F. Welker, M. W. Pedersen, M. E. Allentoft, et al. (2018). Ancient Biomolecules and Evolutionary Inference. Annual review of biochemistry, 87, 1029–1060. Costamagno, S., Théry-Parisot, I., Henry, A. (Eds.), *Gestion des combustibles au Paléolithique et au Mésolithique: nouveaux outils, nouvelles interpretations* (pp. 53-64). BAR International Series 1914. Archaeopress, Oxford.

Mentzer, S. M. (2014). Microarchaeological approaches to the identification and interpretation of combustion features in prehistoric archaeological sites. *Journal of Archaeological Method and Theory, 21*(3), 616–668.

Moucawi, J., Fustec, E., Jambu, P., & Jacquesy, R. (1981). Decomposition of lipids in soils: Free and esterified fatty acids, alcohols and ketones. *Soil Biology & Biochemistry, 13*(6), 461–468.

Munro, N. D., & Bar-Oz, G. (2005). Gazelle bone fat processing in the Levantine Epipalaeolithic. *Journal of Archaeological Science, 32*(2), 223–239.

Munro, L. E., Longstaffe, F. J., & White, C. D. (2007). Burning and boiling of modern deer bone: Effects on crystallinity and oxygen isotope composition of bioapatite phosphate. *Palaeogeography, Palaeoclimatology, Palaeoecology, 249*, 90–102.

Nawar, W. W. (1969). Thermal degradation of lipids. *Journal of Agricultural and Food Chemistry, 17*(1), 18–21.

O'Connell, J. F., Hawkes, K., & Jones, N. B. (1988). Hadza hunting, butchering, and bone transport and their archaeological implications. *Journal of Anthropological Research, 44*(2), 113–161.

Odgaard, U. (2003). Hearth and home of the Palaeo-Eskimos. *Études/Inuit/Studies, 27*(1–2), 349–374.

Outram, A. K. (1999). A comparison of paleo-eskimo and medieval Norse bone fat exploitation in western Greenland. *Arctic Anthropology, 36*(1/2), 103–117.

Outram, A. K. (2001). A new approach to identifying bone marrow and grease exploitation: Why the "indeterminate" fragments should not be ignored. *Journal of Archaeological Science, 28*(4), 401–410.

Outram, A. K. (2002). Identifying dietary stress in marginal environments: Bone fats, optimal foraging theory and the seasonal round. In M. Mondini, S Muiioz & S Wickler (Eds.). *Colonization, migration, and marginal areas: A zooarchaeological approach* (pp. 71–85). Proceedings of the 9th ICAZ Conference, Durham 2002.

Passi, S., Picardo, M., De Luca, C., Nazzaro-Porro, M., Rossi, L., & Rotilio, G. (1993). Saturated dicarboxylic acids as products of unsaturated fatty acid oxidation. *Biochimica et Biophysica Acta, 1168*(2), 190–198.

Pavao-Zuckerman, B. (2011). Rendering economies: Native American labor and secondary animal products in the eighteenth-century Pimería Alta. *American Antiquity, 76*(1), 3–23.

Pettersen, R. C. (1984). The chemical composition of wood. In *The chemistry of solid wood* (Vol. 207, pp. 57–126). Washington: American Chemical Society.

Pham, T. N., Sooknoi, T., Crossley, S. P., & Resasco, D. E. (2013). Ketonization of carboxylic acids: Mechanisms, catalysts, and implications for biomass conversion. *ACS Catalysis, 3*(11), 2456–2473.

Poole, I., Braadbaart, F., Boon, J. J., & van Bergen, P. F. (2002). Stable carbon isotope changes during artificial charring of propagules. *Organic Geochemistry, 33*(12), 1675–1681.

Prost, D., Langevin, O., Lucquin, A., March, R. J., Verdin, P., & D., A. la C. de L. (2011). Le site Néolithique récent-final de "La Garenne" à Gaillon (Eure) et ses structures de combustion. *Revue archéologique de Picardie, numéros spéciaux, 28*, 221–248.

Quigg, J. M. (1997). Bison processing at the rush site, 41TG346, and evidence for pemmican production in the southern plains. *Plains Anthropologist, 42*(159), 145–161.

Rasmussen, K. (1931). The Netsilik Eskimos: Social life and spiritual culture. Report of the Fifth Thule Expedition, 1921-24, Vol. VIII, No. 1-2., Gyldendalske Boghandel, Copenhagen.

Raven, A. M., van Bergen, P. F., Stott, A. W., Dudd, S. N., & Evershed, R. P. (1997). Formation of long-chain ketones in archaeological pottery vessels by pyrolysis of acyl lipids. *Journal of Analytical and Applied Pyrolysis, 40-41*, 267–285.

Regert, M. (2011). Analytical strategies for discriminating archeological fatty substances from animal origin. *Mass Spectrometry Reviews, 30*(2), 177–220.

Reidsma, F. H., van Hoesel, A., van Os, B. J. H., Megens, L., & Braadbaart, F. (2016). Charred bone: Physical and chemical changes during laboratory simulated heating under reducing conditions and its relevance for the study of fire use in archaeology. *Journal of Archaeological Science: Reports, 10*, 282–292.

Renz, M. (2005). Ketonization of carboxylic acids by decarboxylation: Mechanism and scope. *European Journal of Organic Chemistry, 2005*(6), 979–988.

Rottländer, R. C. A. (1989). Chemische untersuchungen an sedimenten der Höhle Geissenklösterle bei Blaubeuren. *Fundberichte Aus Baden-Württemberg, 14*, 23–32.

Rottländer, R. C. A. (1991). Die resultate der modernen Fettanalytik und ihre Anwendung auf die prähistorische Forschung. *Archaeo-Physika, 12*, 1–354.

Ryan, C., McHugh, B., Trueman, C. N., Harrod, C., Berrow, S. D., & O'Connor, I. (2012). Accounting for the effects of lipids in stable isotope (δ13C and δ15N values) analysis of skin and blubber of balaenopterid whales. *Rapid communications in mass spectrometry: RCM, 26*(23), 2745–2754.

Saranpää, P., & Nyberg, H. (1987). Lipids and sterols of *Pinus sylvestris L.* sapwood and heartwood. *Trees, 1*(2), 82–87.

Schiegl, S., Goldberg, P., Pfretzschner, H.-U., & Conard, N. J. (2003). Paleolithic burnt bone horizons from the Swabian Jura: Distinguishing between in situ fireplaces and dumping areas. *Geoarchaeology, 18*(5), 541–565.

Schirmer, A., Rude, M. A., Li, X., Popova, E., & del Cardayre, S. B. (2010). Microbial biosynthesis of alkanes. *Science, 329*(5991), 559–562.

Schwab, A. W., Dykstra, G. J., Selke, E., Sorenson, S. C., & Pryde, E. H. (1988). Diesel fuel from thermal decomposition of soybean oil. *Journal of the American Oil Chemists' Society, 65*(11), 1781–1786.

Shahidi, F. (2005). *Bailey's industrial oil and fat products* (Vol. 6). New York: Wiley-Interscience.

Simoneit, B. R. T. (2002). Biomass burning—A review of organic tracers for smoke from incomplete combustion. *Applied Geochemistry: Journal of the International Association of Geochemistry and Cosmochemistry, 17*(3), 129–162.

Sistiaga, A., Mallol, C., Galván, B., & Summons, R. E. (2014). The Neanderthal meal: A new perspective using faecal biomarkers. *PLoS One, 9*(6), 1–6.

Snoeck, C., Lee-Thorp, J. A., & Schulting, R. J. (2014). From bone to ash: Compositional and structural changes in burned modern and archaeological bone. *Palaeogeography, palaeoclimatology,palaeoecology, 416*, 55–68.

Speth, J. D., & Spielmann, K. A. (1983). Energy source, protein metabolism, and hunter-gatherer subsistence strategies. *Journal of Anthropological Archaeology, 2*(1), 1–31.

Srivastava, A., & Prasad, R. (2000). Triglycerides-based diesel fuels. *Renewable and Sustainable Energy Reviews, 4*(2), 111–133.

Steele, V. J., Stern, B., & Stott, A. W. (2010). Olive oil or lard?: Distinguishing plant oils from animal fats in the archeological record of the eastern Mediterranean using gas chromatography/combustion/isotope ratio mass spectrometry. *Rapid communications in mass spectrometry: RCM, 24*(23), 3478–3484.

Stiner, M. C. (2003). Zooarchaeological evidence for resource intensification in Algarve, southern Portugal. *Promontoria, 1*, 27–61.

Stiner, M. C., Kuhn, S. L., Weiner, S., & Bar Yosef, O. (1995). Differential burning, recrystallization, and fragmentation of archaeological bone. *Journal of Archaeological Science, 22*(2), 223–237.

Stoops, G., & Vepraskas, M. J. (2003). *Guidelines for analysis and description of soil and regolith thin sections*. Fitchburg: Soil Science Society of America.

Surovell, T. A., & Stiner, M. C. (2001). Standardizing infra-red measures of bone mineral crystallinity: An experimental approach. *Journal of Archaeological Science, 28*(6), 633–642.

Théry-Parisot, I. (2002). Fuel management (bone and wood) during the Lower Aurignacian in the Pataud rock shelter (Lower Palaeolithic, Les Eyzies de Tayac, Dordogne, France). Contribution of experimentation. *Journal of Archaeological Science, 29*(12), 1415–1421.

Vajdi, M., Nawar, W. W., & Merritt, C. (1981). GC/MS analysis of some long chain esters, ketones and propanediol diesters. *Journal of the American Oil Chemists' Society, 58*(2), 106–110.

Vehik, S. C. (1977). Bone fragments and bone grease manufacturing: A review of their archaeological use and potential. *Plains Anthropologist, 22*(77), 169–182.

Villa, P., Bon, F., & Castel, J. C. (2002). Fuel, fire and fireplaces in the Palaeolithic of Western Europe. *The Review of Archaeology, 23*(1), 33–42.

Villa, P., Castel, J.-C., Beauval, C., Bourdillat, V., & Goldberg, P. (2004). Human and carnivore sites in the European Middle and Upper Paleolithic: Similarities and differences in bone modification and fragmentation. *Revue de Paléobiologie., 23*, 705–730.

Villagran, X. S., Schaefer, C. E. G. R., & Ligouis, B. (2013). Living in the cold: Geoarchaeology of sealing sites from Byers Peninsula (Livingston Island, Antarctica). *Quaternary International, 315*, 184–199.

Walton, T. J. (1990). Waxes, cutin, and suberin. In J. L. H. JL & J. R. Bowyer (Eds.), *Methods in plant biochemistry* (Vol. 4, pp. 105–158). San Diego: Academic.

Wiedemeier, D. B., Abiven, S., Hockaday, W. C., Keiluweit, M., Kleber, M., Masiello, C. A., McBeath, A. V., Nico, P. S., Pyle, L. A., Schneider, M. P. W., Smernik, R. J., Wiesenberg, G. L. B., & Schmidt, M. W. I. (2015). Aromaticity and degree of aromatic condensation of char. *Organic Geochemistry, 78*, 135–143.

Wiesenberg, G. L. B., Lehndorff, E., & Schwark, L. (2009). Thermal degradation of rye and maize straw: Lipid pattern changes as a function of temperature. *Organic Geochemistry, 40*(2), 167–174.

Yellen, J. E. (1991). Small mammals: !Kung San utilization and the production of faunal assemblages. *Journal of Anthropological Archaeology, 10*(1), 1–26.

Yravedra, J., & Uzquiano, P. (2013). Burnt bone assemblages from El Esquilleu cave (Cantabria, northern Spain): Deliberate use for fuel or systematic disposal of organic waste? *Quaternary Science Reviews, 68*, 175–190.

Zinkel, D. F. (1989). Fats and fatty acids. In J. W. Rowe (Ed.), *Natural products of woody plants* (Springer Series in Wood Science). Berlin: Springer.

Affiliations

Tammy Buonasera [1,2] · Antonio V. Herrera-Herrera [1] · Carolina Mallol [1]

✉ Tammy Buonasera
tybuonasera@gmail.com

Antonio V. Herrera-Herrera
avherrer@ull.edu.es

Carolina Mallol
cmallol@ull.edu.es

[1] Archaeological Micromorphology and Biomarkers (AMBI Lab), Instituto Universitario de Bio-Orgánica Antonio González, Avenida Astrofísico Francisco Sánchez, 38206 La Laguna, Tenerife, Spain

[2] Department of Anthropology, University of California, Davis, One Shields Ave., Davis, CA 95616, USA